

A Survey on Global LiDAR Localization: Challenges, Advances and Open Problems

Huan Yin¹, Xuecheng Xu², Sha Lu², Xieyuanli Chen³,
Rong Xiong², Shaojie Shen¹, Cyrill Stachniss³, Yue Wang^{2*}

¹Department of Electronic and Computer Engineering, Hong Kong
University of Science and Technology, Hong Kong SAR, China.

²College of Control Science and Engineering, Zhejiang University,
Hangzhou, Zhejiang, China.

³Lab for Photogrammetry and Robotics, University of Bonn, Germany.

*Corresponding author(s). E-mail(s): ywang24@zju.edu.cn;

Contributing authors: eehyin@ust.hk; xuechengxu@zju.edu.cn;
lusha@zju.edu.cn; chenxieyuanli@nudt.edu.cn; rxiong@zju.edu.cn;
eeshaojie@ust.hk; cyrill.stachniss@igg.uni-bonn.de;

Abstract

Knowledge about the own pose is key for all mobile robot applications. Thus pose estimation is part of the core functionalities of mobile robots. Over the last two decades, LiDAR scanners have become the standard sensor for robot localization and mapping. This article provides an overview of recent progress and advancements in LiDAR-based global localization. We begin by formulating the problem and exploring the application scope. We then present a review of the methodology, including recent advancements in several topics, such as maps, descriptor extraction, and consistency checks. The contents of the article are organized under three themes. The first theme concerns the combination of global place retrieval and local pose estimation. The second theme is upgrading single-shot measurements to sequential ones for sequential global localization. Finally, the third theme focuses on extending single-robot global localization to cross-robot localization in multi-robot systems. We conclude the survey with a discussion of open challenges and promising directions in global LiDAR localization. To our best knowledge, this is the first comprehensive survey on global LiDAR localization for mobile robots.

Keywords: LiDAR Point Cloud, Global Localization, Place Recognition, Pose Estimation

Contents

1	Introduction	3
1.1	Problem Formulation and Paper Organization	4
1.2	Typical Situations	6
1.2.1	Loop Closure Detection	6
1.2.2	Re-localization	6
1.2.3	Cross-robot Localization	8
1.3	Relationship to Previous Surveys	8
2	Maps for Global Localization	9
2.1	Keyframe-based Submap	9
2.2	Global Feature Map	10
2.3	Global Metric Map	10
3	Single-shot Global Localization:	
	Place Recognition and Pose Estimation	11
3.1	Place Recognition Only	12
3.1.1	Dense Points or Voxels-based	14
3.1.2	Sparse segments-based	16
3.1.3	Projection-based	16
3.2	Place Recognition Followed by Local Pose Estimation	17
3.2.1	Correspondence-based	18
3.2.2	Correspondence-free	20
3.3	Pose Estimation-coupled Place Recognition	21
3.3.1	3-DoF pose estimation	21
3.3.2	6-DoF pose estimation	22
3.4	One-stage Global Pose Estimation	24
3.4.1	Feature-based matching	24
3.4.2	Deep regression	25
4	Global Localization using Sequential Measurements	26
4.1	Sequential Place Matching	26
4.2	Sequential-Metric Localization	28
5	LiDAR-aided Cross-Robot Localization	29
6	Open Problems	33
6.1	Evaluation Difference	33
6.2	Multiple Modalities	34
6.3	Less Overlap	35
6.4	Generalization Ability	36
7	Conclusion	37

1 Introduction

Autonomous navigation is essential for a wide range of mobile robot applications, including self-driving vehicles on roads [Liu et al \(2021\)](#) and agricultural robots in farming [Pretto et al \(2020\)](#). To achieve this, robot localization plays an indispensable role in virtually any navigation system. Today’s tasks of mobile robots require these systems to operate in large-scale and constantly changing environments, posing potential challenges to robot localization and mapping.

The Global Navigation Satellite System (GNSS) is a widely used facility for robot navigation outdoors. GNSS facilitates robot localization primarily in two aspects. First, GNSS-fused methods can track the robot’s *local* motion continuously with limited error, such as GNSS-aided simultaneous localization and mapping (SLAM) [Cao et al \(2022\)](#). The other underlying aspect is that GNSS can provide information on *global* position. This information can help the robot initialize its position on Earth and recover its position if robot localization fails. In fact, both aspects are related to the two typical localization problems: *pose tracking* and *global localization*, which are introduced in the well-known Probabilistic Robotics [Thrun \(2002\)](#). Unlike the pose tracking problem, global localization requires a robot to globally localize itself on a given map from scratch. Thus, the pose space is generally larger than that in the pose tracking problem, resulting in a challenging problem to solve.

GNSS heavily relies on the quality of data sent from satellites, making it impractical in GNSS-unfriendly areas, such as indoors, dense urban environments, or forests. In such environments, ultra-wideband (UWB) and other signal emitters [Ito et al \(2014\)](#) can be deployed for global localization. External markers and tags [Olson \(2011\)](#) can also provide global position and orientation information for visual-aided localization. These methods rely on the distribution of external infrastructures, and modifying the environment is often not desirable. Using onboard sensors without environment modification is a more general solution for mobile robots. Visual images are information-rich and easily obtained from cameras. Early approaches use cameras to achieve global visual localization [Lowry et al \(2015\)](#). Global visual localization is a topic of significant relevance and has attracted lots of research interest [Garg et al \(2021\)](#).

Light detection and ranging (LiDAR) sensors have seen significant development in the last 25 years. Early laser scanners only provided 2D laser points with low resolution and range [Thrun \(2002\)](#). The development of sensor technology has propelled LiDAR sensing from 2D to 3D and from sparse to relatively dense point clouds. In the 2007 DARPA Urban Challenge, the Velodyne HDL-64E sensor was mounted on five of the six automated vehicles that completed the race [Buehler et al \(2009\)](#). LiDAR sensors are now becoming standard equipment in the robotics community. LiDAR sensors directly provide distance measurements by emitting and receiving light. Compared to visual images from cameras, these long-range measurements are more robust to illumination and appearance changes, making global LiDAR localization more practical in large-scale and constantly changing environments. This motivates us to provide a comprehensive review of global localization using LiDAR sensors.

1.1 Problem Formulation and Paper Organization

Given a prior map \mathbf{M} and input data \mathbf{D} , the estimation of robot states (poses) \mathbf{X} can be formulated as follows using the Bayes rule,

$$\hat{\mathbf{X}} = \arg \max_{\mathbf{X}} p(\mathbf{X} | \mathbf{D}, \mathbf{M}) = \arg \max_{\mathbf{X}} p(\mathbf{D} | \mathbf{X}, \mathbf{M}) p(\mathbf{X} | \mathbf{M}) \quad (1)$$

in which $p(\mathbf{X} | \mathbf{D}, \mathbf{M})$ is the likelihood of given poses and map; $p(\mathbf{X} | \mathbf{M})$ is the prior information of \mathbf{X} . The map \mathbf{M} is a critical factor for robot localization, and classical localization-oriented LiDAR maps are introduced in [Section 2](#) before surveying concrete localization methods. Specifically, the LiDAR maps are categorized into three types: keyframe-based submap in [Section 2.1](#), global feature map in [Section 2.2](#) and global metric map in [Section 2.3](#).

For *local pose tracking*, the prior distribution $p(\mathbf{X} | \mathbf{M})$ generally follows a specific non-uniform distribution such as $p(\mathbf{X}) \sim \mathcal{N}(\cdot)$. However, for *global localization*, which aims to achieve state estimation without prior pose information, $p(\mathbf{X} | \mathbf{M})$ follows a uniform distribution, i.e., $p(\mathbf{X} | \mathbf{M}) = \frac{1}{|\mathbf{X}|}$. The resulting estimation problem is given by:

$$\hat{\mathbf{X}} = \arg \max_{\mathbf{X}} p(\mathbf{D} | \mathbf{X}, \mathbf{M}) \quad (2)$$

which is a general formulation of the global localization problem on a given map. The solution space is actually much larger than the local pose tracking problem, making it more challenging.

We start this problem with a single input and a single output. If \mathbf{D} is a single LiDAR point cloud \mathbf{z}_t at timestamp t , the problem is to estimate one global pose \mathbf{x}_t . This problem is referred to as a *single-shot* global localization problem and is comprehensively reviewed in [Section 3](#) of this survey. The single-shot global localization problem can be formulated as a Maximum Likelihood Estimation (MLE) problem as follows:

$$\hat{\mathbf{x}}_t = \arg \max_{\mathbf{x}} p(\mathbf{z}_t | \mathbf{x}_t, \mathbf{M}) \quad (3)$$

In [Section 3](#), we further classify single-shot methods based on the coupling degree of two different approaches: *place recognition* and *pose estimation*, which are two main categories of methods of this survey. Intuitively, place recognition achieves global localization in a retrieval manner while pose estimation provides a fine-grained metric pose. The coupling degree increases sequentially in [Section 3.1](#), [Section 3.2](#), [Section 3.3](#), and [Section 3.4](#). The processing of LiDAR measurement \mathbf{z}_t and the form of the global map \mathbf{M} also vary accordingly in these subsections. A detailed illustration is presented at the beginning of [Section 3](#) and [Figure 3](#).

It is worth noting that the measurement \mathbf{z}_t could be one collected LiDAR *scan* at one timestamp [Chen et al \(2020a\)](#) or one accumulated LiDAR *submap* while the robot moves [Dube et al \(2020\)](#). Both of them are described as LiDAR point clouds and can be considered as one measurement for a single-shot global localization system. We do not differentiate between these two measurements, although single-shot global localization with a sparse LiDAR scan is more challenging than with a dense LiDAR submap.

Typically, the size of a LiDAR map is much larger than that of a single LiDAR point cloud, i.e., $|\mathbf{M}| > |\mathbf{z}_t|$, making the single-shot problem hard to solve. To improve the performance of global localization, one direct approach is to use a continuous stream of scans or submaps as measurements, i.e., $\mathbf{D} = \mathbf{Z}_t \triangleq \{\mathbf{z}_{k=1}, \dots, \mathbf{z}_t\}$. Then the original problem is converted to a *sequential* global localization problem, which will be discussed in [Section 4](#) of this survey paper. The sequential global localization problem can be formulated as follows to estimate \mathbf{X}_t :

$$\hat{\mathbf{X}}_t = \arg \max_{\mathbf{X}} \prod_{k=1}^t p(\mathbf{z}_k | \mathbf{x}_k, \mathbf{M}) p(\mathbf{X}_t) \quad (4)$$

in which $p(\mathbf{X}_t)$ contains the prior information, representing the connections of sequential \mathbf{X}_t . This problem can be regarded as solving a sequence of single-shot global localization in a *batch processing* manner, similar to SeqSLAM [Milford and Wyeth \(2012\)](#) for visual global localization. By solving this, global localization can provide a trajectory of robot poses relative to the global map. Note that additional odometry information could help improve the sequential global localization by constraining the pose space [Pepperell et al \(2014\)](#), and the input data is denoted as $\mathbf{D} = \{\mathbf{Z}_t, \mathbf{U}_{t-1}\}$.

However, in many robotic applications, we may only be interested in the final global pose \mathbf{x}_t with sequential input, for example, \mathbf{x}_t as the initial guess for local pose tracking. In this context, sequential global localization can be seen as a Markovian process to estimate \mathbf{x}_t :

$$\hat{\mathbf{x}}_t \propto \underbrace{p(\mathbf{z}_t | \mathbf{x}_t, \mathbf{M})}_{\text{Measurement}} \underbrace{p(\mathbf{x}_t | \mathbf{x}_{t-1}, \mathbf{u}_{t-1})}_{\text{Motion}} \underbrace{p(\mathbf{X}_{t-1})}_{\text{Prior}} \quad (5)$$

in which the measurement model and motion model are related to \mathbf{z}_t and \mathbf{u}_{t-1} , and the prior $p(\mathbf{X}_{t-1})$ is determined by previous recursive inference. This formulation is also known as *recursive filtering* for localization, and one representative work is Monte Carlo localization (MCL) [Dellaert et al \(1999\)](#). Both batch processing and recursive filtering here are the two main branches for robotic state estimation [Barfoot \(2017\)](#).

As observed from the above equations, single-shot $p(\mathbf{z}_t | \mathbf{x}_t, \mathbf{M})$ still plays a key role in the sequential global localization problem. From another perspective, we can also categorize sequential global localization based on the use of place recognition and pose estimation, thus bridging the gap between [Section 3](#) and [Section 4](#). We will introduce sequential place matching methods and sequential-metric methods in [Section 4.1](#) and [Section 4.2](#), respectively. The former mainly utilizes sequential place recognition results and the latter focuses on estimating metric poses. Meanwhile, we also keep the discussion on the line of batch processing and recursive filtering in these two subsections.

[Section 3](#) and [Section 4](#) survey the mainstream methods for global LiDAR localization. In practical situations, global localization methods could not work very well in extreme conditions, such as localizing on an outdated map or localizing a robot on another robot's map. In [Section 5](#), we provide a review of several popular methods

that could improve performance in such conditions, particularly focusing on multi-robot situations. Finally, [Section 6](#), open problems of global LiDAR localization are discussed as a conclusion for future study.

In summary, our paper structure is similar to a fish, as illustrated in [Figure 1](#). [Section 1](#) details the global localization problem and the scope of this survey. We then present three types of map frameworks in [Section 2](#). [Section 3](#) and [Section 4](#) then provide an overview of existing methods based on the number of measurements: single-shot or sequential. The former focuses on matching a single LiDAR point cloud on a given map, while the latter takes sequential measurements to approximate the ground truth pose. Then in [Section 5](#), we extend the global localization problem to the cross-robot localization problem for multi-robot applications. Finally, [Section 6](#) provides discussions about open challenges and emerging issues of global LiDAR localization. A conclusion of this survey is presented in [Section 7](#).

1.2 Typical Situations

The concrete global localization method varies according to actual situations in robot mapping and localization. Three typical situations are illustrated as follows.

1.2.1 Loop Closure Detection

In a SLAM framework, loop closure detection (LCD) is a method used to determine whether a robot has returned to a previously visited location or place. However, simply recognizing revisited locations is insufficient for performing loop closure in SLAM. Typically, the relative transformation between the current and previous locations is also required, as is the case for graph-based consistent mapping methods [Kümmerle et al \(2011\)](#); [Dellaert \(2012\)](#). In this paper, we use the terms LCD and loop closing interchangeably, as both involve detecting revisited locations and estimating relative transformations. LCD is generally regarded as an *intra-sequence* problem, as it involves measurements and a map within the same sequence, and is typically applied to a single-session single-robot scenario.

1.2.2 Re-localization

Re-localization serves to assist a robot in recovering when there is a failure in pose tracking or when the robot has been kidnapped. Additionally, it can be used to activate the robot at the beginning of navigation. The fundamental distinction between loop closure detection (LCD) and re-localization lies in the data sequence used: re-localization is classified as an *inter-sequence* problem, wherein measurements and a map are obtained from different data sequences [Knights et al \(2022b\)](#). It is noteworthy that re-localization can pose significant challenges in the case of long-term multi-session sequences, such as attempting to re-localize a LiDAR scan on an outdated point cloud map. Additionally, the pose space $|\mathbb{X}|$ of re-localization can be larger than that of LCD in some instances since there is no prior information available in re-localization, while LCD may employ odometry information as a crude initial estimate, thereby reducing the pose space to a smaller size.

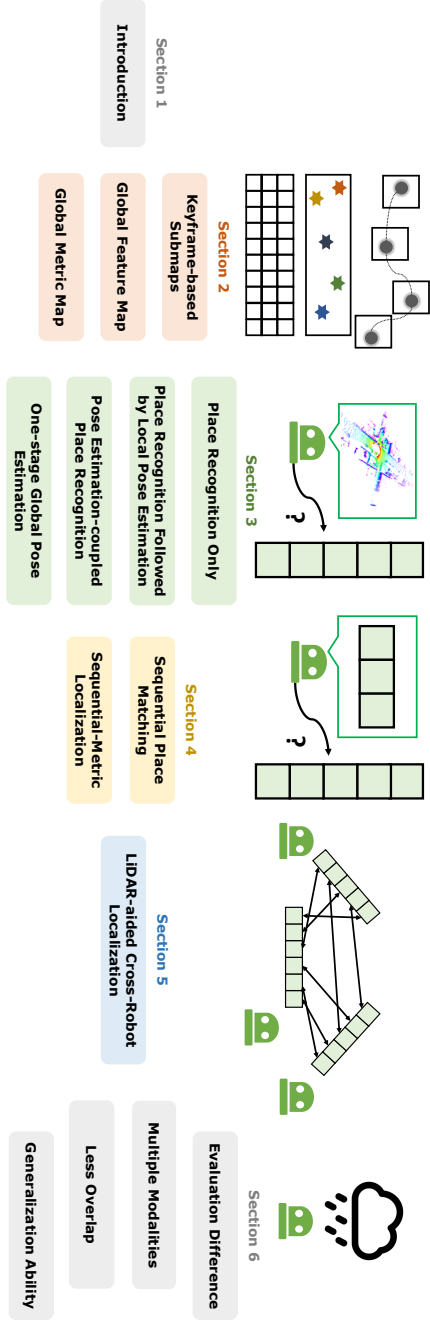


Fig. 1 Fish-shaped paper structure. This survey starts the problem formulation and related introduction at the fish head. Then the fish body part contains the main subtopics of the global LiDAR localization problem: map framework, single-shot and sequential global localization, and cross-robot localization. Finally, an extended discussion on open problems is presented at the fish tail

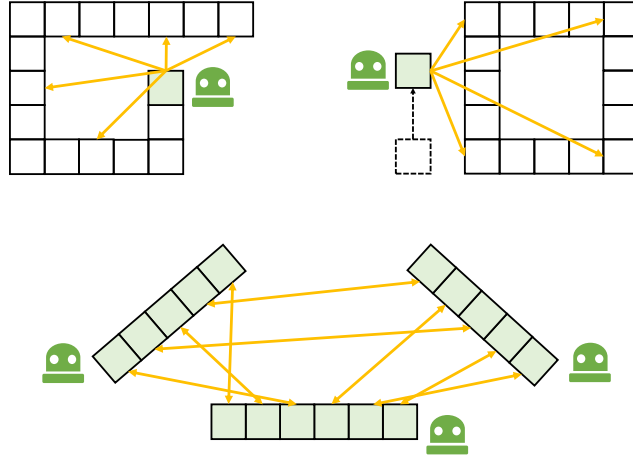


Fig. 2 Three typical situations. From top to down: single-robot intra-sequence LCD (loop closing); single-robot inter-sequence re-localization; cross-robot inter-sequence localization. Green-filled boxes and black border boxes indicate measurements and maps, respectively. Orange lines are possible relative transformations for global localization problems.

1.2.3 Cross-robot Localization

Multiple online maps can be generated from multiple robots using incremental SLAM or other mapping techniques. These maps might be with partial overlap but are under their own coordinate. Cross-robot localization, or multiple-robot mapping, aims to localize a robot globally on another robot’s map. More concretely, \mathbf{D} and \mathbf{M} come from different robots and all robots’ poses are required to be estimated. Theoretically, the cross-robot localization problem is identical to the single-robot re-localization [Thrun \(2002\)](#) but in a *multi-robot* scenario. Relevant techniques can also be employed to offline map merging applications. For instance, cross-robot localization is performed on multiple sessions collected by a single robot for long-term use, while the challenge is that perspective changes may occur under long-term conditions.

Figure 2 illustrates three common scenarios in which a robot needs to estimate relative transformations between its current measurements and its own or another robot’s map. This ability is commonly referred to as global localization, and it can be achieved with various sensors and fused sensor modalities. This survey specifically focuses on the global LiDAR localization problem and the techniques relevant to it.

1.3 Relationship to Previous Surveys

Lowry *et al.* [Lowry et al \(2015\)](#) provide a thorough review on visual place recognition in 2015. They start by discussing the “place” definition and introduce related techniques for visual place recognition. A general place recognition survey [Yin et al \(2022c\)](#) reviews the place recognition topic from multiple perspectives, including sensor modalities, challenges and datasets. However, place recognition determines whether a robot

revisits a previous place by retrieval, which is not equal to the concept of global localization. Toft *et al.* [Toft et al \(2020\)](#) review the long-term visual localization and make evaluations on state-of-the-art approaches, such as visual place recognition (image-retrieval)-based and structure-based camera pose estimation. Elhousni *et al.* [Elhousni and Huang \(2020\)](#) presents a LiDAR localization survey, focusing on LiDAR-aided pose tracking for autonomous vehicles. LiDAR place recognition and pose estimation are not reviewed explicitly in these survey papers [Lowry et al \(2015\)](#); [Yin et al \(2022c\)](#); [Toft et al \(2020\)](#); [Elhousni and Huang \(2020\)](#). From the view of global LiDAR localization, we present a complete survey that covers relevant topics, like the ones [Lowry et al \(2015\)](#); [Toft et al \(2020\)](#) on vision.

Cadena *et al.* [Cadena et al \(2016\)](#) present a history of SLAM and promising research directions in 2016. SLAM has supported various robotic applications. A recent article by Ebadi *et al.* [Ebadi et al \(2022\)](#) surveys recent progress on challenging underground SLAM. Specifically, SLAM aims to incrementally estimate pose and construct maps, while global localization estimates a global pose on a prior map. These two problems have a certain relevance. More concretely, LCD is a key characteristic of modern-day SLAM algorithms, as introduced in the Handbook of Robotics [Stachniss et al \(2016\)](#). The absence of loop closing or place recognition will reduce SLAM to [Cadena et al \(2016\)](#). We believe this survey paper will help users make LiDAR SLAM systems more robust and accurate.

2 Maps for Global Localization

Before delving into the methodology section, it is essential to introduce maps \mathbf{M} for robot localization. This section primarily focuses on maps that support global localization and classifies general-use maps into three primary clusters: keyframe-based submap, global feature map, and global metric map, based on the map’s structure and representations inside.

2.1 Keyframe-based Submap

The keyframe-based submap is a highly popular map structure for robot localization, particularly in large-scale environments. It consists of a set of keyframes, each containing a robot pose and an aligned submap, as well as additional information in the form of topological or geometrical connections between keyframes [Lowry et al \(2015\)](#). Keyframe-based submaps are easy to maintain and well-suited for downstream navigation tasks [Tang et al \(2019\)](#). The keyframe-based map can be represented as:

$$\mathbf{M}_{\text{key}} = \{\mathbf{m}_1, \dots, \mathbf{m}_s\} \quad (6)$$

where s represents the number of submaps. In other words, s corresponds to the size of \mathbb{X} if we only retrieve places in the keyframe database.

A keyframe-based map effectively discretizes the entire pose space, reducing the complexity of the problem. This discrete map structure is particularly well-suited for place retrieval, as each keyframe can be considered a distinct "place" for the mobile robot. The submap contained within each keyframe can serve as a global descriptor

for retrieval or can be augmented with additional metric grids or points for geometric registration. Notably, the distance between keyframe poses is a critical factor in practice. For example, if this distance is large or the keyframe resolution is low, fewer keyframes (i.e., a smaller s) may be needed for lightweight robot navigation, but at the cost of increased risk of localization failure. Additionally, it should be noted that keyframe-based maps may not be suitable for global localization in certain environments, such as indoor or forested areas where many local environments are similar. In such cases, a global map may be preferred.

2.2 Global Feature Map

A global feature map keeps sparse local feature points to describe the environments. Early SLAM systems extract landmarks from laser data to support mapping and localization, like tree trunks in the Victoria Park dataset [Guivant and Nebot \(2001\)](#). These landmarks are essentially low-dimensional feature points. Nowadays, LiDAR feature points are generally with high-dimensional information [Dubé et al \(2017\)](#). Hence, feature correspondence-based matching can be directly used for relative transformation estimation. More importantly, local features are sparse and easy to manage, making the navigation system more lightweight.

The main challenge of applying such maps is generating and maintaining stable feature points. For instance, a high-definition map (HD map) is a typical global feature map for self-driving vehicles. HD-map construction involves multiple onboard sensors and high-performance computation, and maintaining a global HD map is costly. As for the LiDAR-only global feature map, a powerful front-end feature extractor is necessary to ensure the map quality.

2.3 Global Metric Map

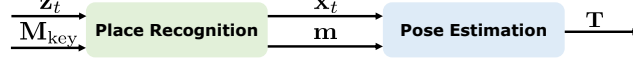
A global metric map is a single map with dense metric representations describing a working environment. Generally, metric and explicit representations include 2D/3D points [Lee et al \(2022\)](#), grids [Hess et al \(2016\)](#), voxels [Wurm et al \(2010\)](#), and meshes [Chen et al \(2021b\)](#). The global metric map is easy to use and can provide high-precision geometric information.

But localization, whether pose tracking or global localization, is only one block in common autonomous navigation systems. In large-scale environments, the global metric map can be a burden for resource-constrained mobile robots. One might suggest that we could downsample or compress dense points while keeping the main geometric property [Labussière et al \(2020\)](#); [Yin et al \(2020\)](#). But as pointed out by [Chang et al \(2021\)](#), localization performances drop as the map size budget decreases using raw points. There are two solutions to tackle this problem: one is to use sparse local features rather than dense representations, i.e., the global feature map; another is to split the map space into submaps, i.e., keyframe-based submaps. Map framework and contents inside should be designed according to the application scenarios.

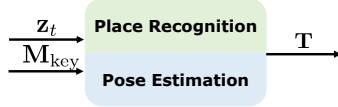
It is worth noting that implicit map representations are becoming highly popular, including non-learning [Saarinen et al \(2013\)](#); [Wolcott and Eustice \(2015\)](#) and learning-based ones [Kuang et al \(2022\)](#). One famous work is normal distribution transform



(a) Section 3.1: Place recognition only



(b) Section 3.2: Place recognition followed by local pose estimation



(c) Section 3.3: Pose estimation-coupled place recognition



(d) Section 3.4: One-stage global pose estimation

Fig. 3 Four types of single-shot global localization. $\mathbf{z}_t = \mathcal{P}$ indicates a single LiDAR point cloud. \mathbf{M}_{key} and $\mathbf{M}_{\text{global}}$ represent keyframe-based submaps and a global metric/feature map respectively. \mathbf{x}_t and $\mathbf{m} = \mathcal{M}$ represent the retrieved robot pose and metric map via place recognition in the keyframe-based submaps. \mathbf{T} is the estimated pose by using relative pose estimation approaches.

(NDT), which uses probability density functions as representations. Implicit representations use fewer parameters compared with explicit ones [Lee et al \(2022\)](#); [Hess et al \(2016\)](#); [Wurm et al \(2010\)](#); [Chen et al \(2021b\)](#).

In summary, three kinds of maps are introduced in this section. These map structures and their representations inside are the foundations that can support global LiDAR localization in the following Section 3 Section 4. Map representation is a basic but critical topic for SLAM and other navigation-related applications. We recommend reading a review by Rosen *et al.* [Rosen et al \(2021\)](#) for readers interested in this topic.

3 Single-shot Global Localization: Place Recognition and Pose Estimation

Single-shot global localization methods solve pose estimation using a *single* LiDAR point cloud only. *Place recognition* is the core backbone to achieve this. Generally, place recognition is a discriminative model based on keyframe-based submaps, in which every keyframe generally consists of a global descriptor and a robot pose. The basic

idea of place recognition is to *retrieve the highest-probability place based on based on global descriptors and measured similarities between \mathbf{z}_t and \mathbf{M}_{key}* . More specifically, these global descriptors should have a certain discriminativeness: be discriminative for different places but keep similar for places close to each other.

However, place recognition can only provide a coarse place as the estimated place, while *pose estimation* is still needed via local feature matching or similar techniques. In this section, we categorize all single-shot approaches considering their degree of place recognition and relative pose estimation, as follows:

- Section 3.1: *Place Recognition Only* approaches retrieve the most similar place using descriptors. The pose of a retrieved place (keyframe) is regarded as the estimated pose. These
- Section 3.2: *Place Recognition Followed by Local Pose Estimation* first achieves place recognition and then estimates the robot pose via a customized pose estimator.
- Section 3.3: *Pose Estimation-coupled Place Recognition* tightly couple the two stages together. Place recognition and pose estimation benefit from shared representations.
- Section 3.4: *One-stage Global Pose Estimation* directly estimates the global pose on a global map using pose estimation, thus no place retrieval and keyframes are required.

We present several representative works of single-shot global LiDAR localization in Table 1. Methods in Section 3.2 are not listed since we mainly introduce LiDAR pose estimation methods in Section 3.2, and these methods can be applied to refine place recognition results.

Figure 3 presents four types of combinations between the place recognition module and the pose estimation module. From the perspective of maps, in Section 3.1, 3.2 and 3.3, methods generally rely on keyframe-based submaps. While in Section 3.4, global localization is generally based on a global metric or feature map.

It is worth noting that the boundaries are not so clear for these four types of approaches. For instance, there are no global descriptors in several place recognition systems Bosse and Zlot (2009). Local feature-based pose estimation plays an important part in place recognition. We consider they lie in the boundary of coupled methods (Section 3.3) and one-stage methods (Section 3.4), and will present them in Section 3.3 for clearance.

3.1 Place Recognition Only

Place recognition-only approaches solve the global localization problem by retrieving places in a pre-built keyframe-based map. Figure 4 presents a place recognition-only approach for better understanding. The challenging part of LiDAR place recognition is the descriptor extraction. Compared to visual images, raw point clouds from LiDAR are textureless and in an irregular format, sometimes with an uneven density. From the perspective of data processing, global descriptor extraction is a kind of compression method for point clouds, while maintaining the distinctiveness of different places. We categorize current LiDAR place recognition based on how to handle LiDAR data pre-processing.

Table 1 Representative Works of Single-shot Global LiDAR Localization. (Section 3.1, 3.3.1, 3.3.2 and 3.4)

Name	Pose	Pre-Processing	Learning	Backbone	Similarity/Loss	Evaluation	Dataset
Röhling et al (2015)	Place	Points	No	Histogram-based	Wasserstein	F1 score, MCC	Self-Collect
Uy and Lee (2018)	Place	Points	Yes	3D PointNet + NetVLAD	Triplet, Quadruplet	Recall@1, Recall@1%	RobotCar, In-house
Komorowski (2021)	Place	Points	Yes	3D Feature Pyramid Network + Generalized-mean Graph Similarity Network	Triplet Margin	Recall@1, Recall@1%	RobotCar, In-house
Kong et al (2020)	Place	Segments	Yes		BCE of Place	F1 score, PRC	Semantic KITTI
He et al (2016)	Place	Projection	No	Multiple planes, Density Signature	Euclidean	Recall (100% Precision), PRC	KITTI, Freiburg Campus, Ford
Yin et al (2022b)	Place	Projection	Yes	Spherical Projection + VLAD Layer	Viewpoint-Quadruplet	Recall@1%, PRC	KITTI, Self-Collect
Kim and Kim (2018)	3-DoF	Projection	No	2D Ring Key, Scan Context	Column-wise Cosine	PRC, RMSE with ICP	KITTI, NCLT, Complex Urban
Xu et al (2021b)	3-DoF	Projection	Yes	Multi-layer Scan Context + CNN + FFT	Quadruplet	PRC, Recall@1(%), Yaw Estimation	RobotCar, NCLT, MulRan
Chen et al (2020a)	3-DoF	Projection	Yes	Multi-layer Range Image + CNN + FFT	Image Overlap, BCE of Yaw angle	PRC, Yaw Estimation	KITTI, Ford Campus
Shan et al (2021)	6-DoF	Projection	No	Range Image + DBow + Feature Matching	L1, Hamming	ROC, LCD with Pose	Self-Collect
Cattaneo et al (2022)	6-DoF	Points	Yes	PV-RCNN + BEV feature map	Triplet + Pose Error + Unbalanced optimal transport	PRC, Pose Error	KITTI, KITTI-360, Self-Collect
Yuan et al (2022)	6-DoF	Points	No	Stable Triangle Descriptor, Hash Key	Similarity of Triangles	PRC, Pose Error	KITTI, NCLT, Complex Urban, Self-Collect
Dubé et al (2017)	6-DoF	Segments	Yes	Handcraft Features + Random Forest + RANSAC	by Matching	ROC, LCD with Pose	KITTI
Wang et al (2021)	6-DoF	Points	Yes	PointNet-style + Self-Attention	Pose Error	Pose Error	RobotCar, Self-Collect

¹ MCC: Matthews Correlation Coefficient, BCE: Binary Cross-Entropy, PRC: Precision-Recall Curve, ROC: Receiver Operating Characteristic

² Only list main evaluation results due to the page size.

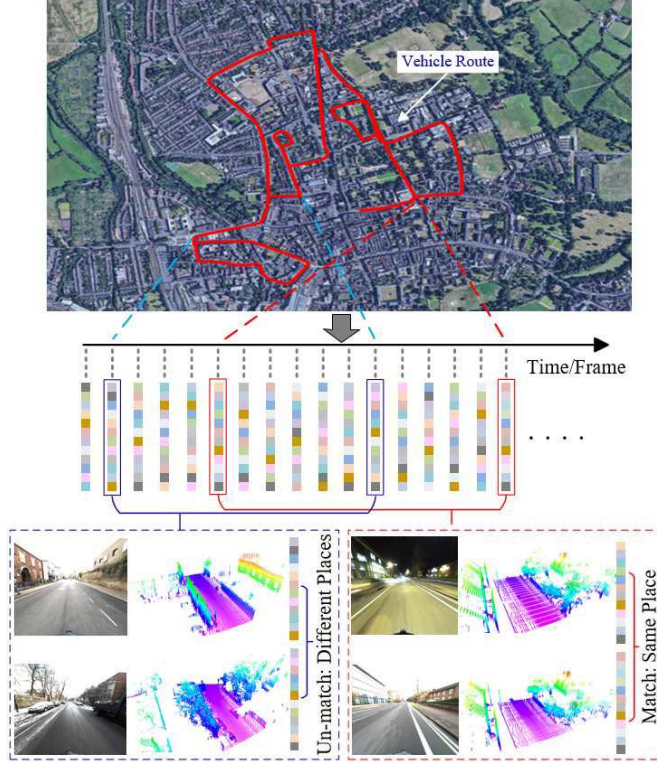


Fig. 4 From LPDNet [Liu et al \(2019b\)](#). LPD-Net is a place recognition-only approach for global LiDAR localization. Global descriptors are extracted as place descriptions for place retrieval.

3.1.1 Dense Points or Voxels-based

Dense points and dense voxels-based works refer to those that generate global descriptors directly on dense representations. Early laser scanners can only provide 2D laser points for robotic localization. [Granström et al. \(2009\)](#) design a global descriptor that consists of 20 features in a 2D laser scan, such as a covered area and a number of clusters in range data. Then handcrafted descriptors and labels are fed into a weak classifier Adaboost [Freund and Schapire \(1997\)](#) for training. The learning-based approach is extended to 3D laser features in [Granström et al \(2011\)](#). Instead of extracting features, Fast Histogram [Röhling et al \(2015\)](#) encodes the range distribution of 3D points into a one-dimensional histogram for place retrieval. Earth Mover’s distance is employed to measure the similarity of different histograms, which differs from Euclidean distance or Cosine distance in most place recognition methods. Inspired by [Röhling et al \(2015\)](#), [Yin et al. \(2017\)](#) build a 2D image-like representation based on divisions of altitude and range in a 3D LiDAR scan. Then the problem can be converted to an image classification problem that can be solved by training a 2D convolutional neural network with a basic contrastive loss [Hadsell et al \(2006\)](#). Aside from using the range information of LiDAR scanners, DELIGHT [Cop](#)

et al (2018) utilizes the histograms of LiDAR intensity as the descriptor for place recognition followed by geometry verification.

All the methods above design handcrafted 2D or 1D histograms for LiDAR-based place recognition. This is because deep learning for 3D point clouds was not so mature then. In 2017, Qi *et al.* Qi et al (2017) proposed PointNet, which can learn local and global features for 3D deep learning tasks. Novel encoders also boost the performance of point cloud processing, like KPconv Thomas et al (2019) for point convolution. PointNetVLAD Uy and Lee (2018) utilizes PointNet to extract features of 3D point clouds and aggregates them into a global descriptor via NetVLAD Arandjelovic et al (2016). But limited by PointNet, PointNetVLAD ignores the local geometry distribution in 3D point clouds. To address this problem, LPDNet Liu et al (2019b) designs an adaptive local feature extraction module based on ten handcrafted local features, and a graph-based neighborhood aggregation module to generate a global descriptor. With the appearance of Transformer Vaswani et al (2017) in diverse tasks to achieve long-range dependencies, the attention mechanism has been increasingly used to select significant local features for place recognition. PCAN Zhang and Xiao (2019) takes local features into account and computes an attention map to determine each feature’s significance. SOE-Net by Xia *et al.* Xia et al (2021) uses a point orientation encoding module to generate point-wise local features and feeds them into a self-attention network aggregating them to a global descriptor. Nevertheless, these methods cannot fully extract the point-wise local features around the neighbors. Hui *et al.* propose a pyramid point cloud transformer network named PPT-Net Hui et al (2021). PPT-Net could learn the local features at different scales and aggregate them to a descriptive global representation by a pyramid VLAD. Recent work Lin et al (2022) utilizes SE(3)-equivariant networks to learn global descriptors, making place recognition more robust to the rotation and translation changes. Despite the network structure design, a local consistency loss is proposed in Vidanapathirana et al (2022) to guarantee the consistency of local features extracted from point clouds at the same place. To save memory and improve transmission efficiency, Wiesmann *et al.* Wiesmann et al (2022a) propose a compressed point cloud representation aggregated by an attention mechanism for place recognition. Authors also design a novel architecture for more efficient training and inference in Wiesmann et al (2022b).

Another popular pipeline is to voxelize the 3D point clouds first, and then extract global descriptors for place recognition. The voxelizing process can make the raw 3D point clouds more regular. This makes 3D point clouds close to 3D image-like representations, i.e., each grid (2D) or cube (3D) can be regarded as one image patch. Magnusson *et al.* Magnusson et al (2009a,b) classify local cells into planes, lines and spheres, and then aggregate them all into a vector as a global descriptor for place recognition. The classification criteria are based on the local distributed probability density function, i.e., NDT. In the deep learning age, Zhou *et al.* Zhou et al (2021) propose NDT-Transformer, which transforms the raw point cloud into NDT cells and uses the attention module to enhance the discrimination. VBRL proposed by Siva *et al.* Siva et al (2020) introduces a voxel-based 3D representation that combines multi-modal features in a regularized optimization formulation. Oertel *et al.* proposes AugNet Oertel et al (2020), an augmented image-based place recognition method

that combines appearance and structure features. Komorowski *et al.* introduce MinkLoc3D Komorowski (2021), which extracts local features on a sparse voxelized point cloud by feature pyramid network and aggregates them into a global descriptor by pooling operations. After that, they propose MinkLoc3Dv2 Komorowski (2022) as the enhancement of MinkLoc3D Komorowski (2021), which leverages deeper and wider network architecture with an improved training process.

3.1.2 Sparse segments-based

Segmentation-based approaches refer to works that perform place recognition based on point segments, which leverage the advantages of both local and global representations. Seed Fan *et al.* (2020) segments the raw point cloud to segmented objects and encodes the topological information of these objects into the descriptor. SGPR Kong *et al.* (2020) proposed by Kong *et al.* exploits both semantic and topological information of the raw point cloud and uses a graph neural network to generate the semantic graph representation. Locus Vidanapathirana *et al.* (2021) encodes the temporal and topological information to a global descriptor as a discriminative scene representation. Gong *et al.* Gong *et al.* (2021) utilize spatial relations of segments in both high-level descriptors search and low-level geometric search. Overall, segmentation-based approaches are close to what our human beings think about place recognition, i.e., using high-level representations rather than low-level geometry. On the other hand, these methods heavily rely on the segmentation quality and other additional semantic information. 3D point cloud segmentation approaches have typically been time-consuming and resource intensive.

3.1.3 Projection-based

Projection-based methods, in contrast to the aforementioned two categories, do not generate the descriptor directly on 3D point clouds or segments; instead, these methods project a 3D point cloud to 2D planes first and then achieve global descriptor extraction. He *et al.* He *et al.* (2016) propose M2DP that projects the raw point cloud into multiple 2D planes, constructing the signature with descriptors from different planes. LiDAR Iris Wang *et al.* (2020b) encodes the height information of a 3D point cloud into a binary LiDAR-Iris image and converts it into a Fourier domain to achieve rotation invariance. RINet proposed by Kong *et al.* Li *et al.* (2022) converts a point cloud to a scan context image encoded by semantic information first and designs a rotation-invariant network for learning a rotation-invariant representation. Yin *et al.* Yin *et al.* (2022b) propose a multi-layer spherical projection via discrete 3D space. Then VLAD layer Arandjelovic *et al.* (2016) and spherical convolutions Cohen *et al.* (2018) are integrated as SphereVLAD based on spherical projections. SphereVLAD can learn a viewpoint-invariant global descriptor for place recognition.

Summary. Early approaches in Section 3.1.1 and 3.1.3 tried to design handcrafted global descriptors from a traditional data processing viewpoint. With the development of neural network techniques, data-driven descriptors are becoming more and more popular, resulting in high performance on place recognition (>95% on Recall@1 in Xu *et al.* (2021a); Komorowski (2022)). Several approaches have achieved fully rotation-invariant descriptors for place retrieval, like handcrafted Fast Histogram in Röhling

et al (2015) and learning-based SphereVLAD in Yin et al (2022b). We can conclude that global descriptor extraction of 3D LiDAR point clouds has reached a level of success. However, there still remain several challenges and issues, e.g., generalization ability, that will discuss in Section 6.4.

All the methods in this subsection only provide retrieved places as output. The global localization performance is evaluated under machine learning metrics, like precision-recall curves and F-1 score. In this context, the translation precision of pose (place) is decided by the resolution of keyframes (25m for evaluation on Oxford RobotCar Dataset Maddern et al (2017)); the precision of rotation estimation is not considered or evaluated. In practice, this actually can not meet the demand of most high-precision global localization tasks, e.g., building a consistent global map with relative transformations, or waking the robot up with a precise location.

From another point of view, global descriptors are highly compressed representations of raw LiDAR data, and there exists information loss in the compression process, especially for those end-to-end deep learning methods. This kind of representation is naturally suitable for nearest neighbor search in place retrieval but can not be used in geometric pose estimation. In the following section, we present a review of the local transformation estimation that metric representation involves.

3.2 Place Recognition Followed by Local Pose Estimation

This section reviews local pose estimation methods for high-precision transformation estimation. Note that this local pose estimation is independent of place recognition in this subsection. These two components are seen as separated and the global localization is achieved in a coarse-to-fine manner: first achieve place retrieval on keyframe-based submaps, then apply local pose estimation via matching input LiDAR to map data attached on the retrieved keyframe. Hence, for this group of approaches, the keyframe includes not only global descriptors for nearest neighbor search (place retrieval), but also metric representations for local pose estimation. Conventionally, the local pose estimation is achieved by precise point cloud registration.

Point cloud registration, or named scan matching, is a popular topic in robotics and computer vision. It aims at estimating the optimal transformation by minimizing the error function as follows:

$$\mathbf{T} = \arg \min_{\mathbf{T} \in \text{SE}(3)} (e(\mathcal{M}, \mathbf{T}\mathcal{P})), \quad (7)$$

in which \mathbf{T} is the relative transformation (pose) to be estimated; \mathcal{P} and \mathcal{M} are the source points (input LiDAR measurement \mathbf{z}_t) and target points (prior map in the retrieved keyframe \mathbf{m}) respectively; $e(\cdot)$ is an error function to minimize. This subsection mainly focuses on the *global* point cloud registration. Specifically, point cloud registration approaches can be categorized into two types based on whether using correspondences between these two point clouds.

3.2.1 Correspondence-based

If correspondences (data associations) between query measurements and map are known, the registration problem can be solved in a closed form [Horn \(1987\)](#); [Arun et al \(1987\)](#). Unfortunately, the initial correspondences are unknown in practice. The most well-known algorithm to scan registration is Iterative Closest Point (ICP) [Besl and McKay \(1992\)](#), which considers a basic point-to-point correspondence search and finds the optimal solution at each iteration. The ICP family follows an expectation-maximization framework that alternates between finding correspondence and optimizing pose. Despite its widespread use in point cloud registration, the quality of the registration result is limited by the presence of noise and outliers. An effective real-time registration system based on ICP is KISS-ICP [Vizzo et al \(2022\)](#). To improve the original ICP algorithm, many variants have been designed. Probabilistic methods Generalized-ICP [Segal et al \(2009\)](#) and NDT [Biber and Straßer \(2003\)](#) define Gaussian models for points or voxels and perform registration in a distribution-to-distribution manner, therefore reducing the influence of noise. We recommend interested readers consider a registration review for mobile robotics [Pomerleau et al \(2015\)](#).

However, ICP and its variants might fall into local minima, making it inapplicable for global registration. Go-ICP by Yang *et al.* [Yang et al \(2013\)](#) provides a global solution to the registration problem defined by ICP in 3D using branch-and-bound (BnB) theory. Go-ICP, however, is time-consuming on resource-constrained platforms, especially when the pose space is large for BnB search. If the transformation is in a limited space, BnB-based scan matching is more efficient to use, like LCD in Cartographer [Hess et al \(2016\)](#) and vehicular pose tracking on a Gaussian mixture maps [Wolcott and Eustice \(2015\)](#).

For ICP and its variants, the local minima are caused by the assumption of nearest-neighbor correspondence in Euclidean space. Local feature-based approaches have emerged to extract robust features for correspondence search in a feature space. With the correspondence determined, the transformation can be calculated in the closed form, or with an additional outlier filter. But compared to 2D image descriptors like SIFT [Lowe \(1999\)](#) or ORB [Rublee et al \(2011\)](#), the study on LiDAR feature extraction and description is less extensive. The nature of range data is different from image data. Extracting and describing repeatable features in LiDAR scans is still an open problem. The less accurate correspondences provided by feature matching will cause a much higher outlier rate than their 2D counterparts. To address these issues, there are mainly two lines of research in recent years: one is to study the effective LiDAR features; the other is to configure a robust estimator that can handle high outlier rates. We will address these two lines as follows.

The feature extraction of 2D laser scans follows the pipeline in computer vision: first detect interest points (keypoints), and then compute a distinctive signature for each of them (local descriptors) [Nielsen and Hendeby \(2022\)](#). Tipaldi and Arras [Tipaldi and Arras \(2010\)](#) propose a fast laser interest region transform (FLIRT) for feature extraction, which adopts the theory in SIFT [Lowe \(1999\)](#). FALKO [Kallasi et al \(2016\)](#) is also an effective keypoint detection that specialized in 2D range data. BID by Usman *et al.* [Usman et al \(2019\)](#) uses B-spline to fit the data along keypoints that are detected by FALKO [Kallasi et al \(2016\)](#). Then the spline is formulated into the descriptors for

feature matching. As for 3D range data, early approaches to extract 3D features are mainly handcrafted [Guo et al \(2016\)](#), such as FPFH [Rusu et al \(2009\)](#), NARF [Steder et al \(2010b\)](#) and SHOT [Salti et al \(2014\)](#). These methods are designed for dense point clouds obtained by RGBD cameras, which lack generalization and robustness against noise. Deep learning has drawn much attention in recent years, and many learning-based features have been proposed. 3DMatch [Zeng et al \(2017\)](#) takes 3D local patches around arbitrary interest points and extracts 3D features using a 3D convolutional neural network. PPF-net [Deng et al \(2018\)](#) utilizes PointNet [Qi et al \(2017\)](#) to extract local patch features and further fuse the global context into this feature. FCGF [Choy et al \(2019\)](#) utilizes a fully convolutional network to capture global information. It also adopts sparse convolution to efficiently extract local features.

These methods focus on the local feature extraction from interest points; however, interest point or keypoint detection is also important. The stable keypoints that are highly repeatable on 3D point clouds under arbitrary transformation are essential for the registration task. There is a comprehensive review of 3D keypoint detection that evaluates most handcrafted 3D keypoints [Tombari et al \(2013\)](#). The common trait of these methods is their reliance on local geometric information, which discards the important global context. To address these problems, USIP [Li and Lee \(2019\)](#) proposes an unsupervised framework to detect keypoints. SKD [Tinchev et al \(2021\)](#) uses saliency estimation to determine the keypoints. Some works [Yew and Lee \(2018\)](#); [Bai et al \(2020\)](#) also jointly learn the keypoint detector and descriptor.

The limitation of correspondence-based methods is the robustness of the estimator with respect to outliers and low overlaps. Then we shift from the “3D features” line to the “robust estimator” line. Several research works tried to address this problem from different perspectives. Random sample consensus (RANSAC) [Fischler and Bolles \(1981\)](#) is a widely used robust estimator for outlier pruning. FGR [Zhou et al \(2016\)](#) regards this problem as an optimization problem. FGR implements a Geman-McClure cost function and leverages second-order optimization to reach global registration of high accuracy. DGR [Choy et al \(2020\)](#) proposes a differentiable Weighted Procrustes algorithm for closed-form pose estimation and a robust gradient-based SE(3) optimizer for pose refinement. TEASER by Yang *et al.* [Yang et al \(2021\)](#) is the first certifiable registration algorithm that can achieve acceptable results with a large percentage of outliers. A powerful maximum clique finder [Eppstein et al \(2010\)](#) is an important module for handling outliers in TEASER. With pruned correspondences, graduated nonconvexity [Yang et al \(2020\)](#) is then used for robust pose estimation. Actually, the *maximum clique* problem can also be formulated as a graph-theoretic optimization problem. Parker *et al.* [Lusk et al \(2021\)](#) present CLIPPER to solve this optimization by continuous relaxation. PointDSC [Bai et al \(2021\)](#) utilizes a spatial-consistency guided nonlocal module for feature learning and proposes a differentiable neural spectral matching for outlier removal. Different robust kernels are considered for point cloud registration. An elegant formulation based on Barron’s kernel family [Barron \(2019\)](#) has been proposed by Chebrolu *et al.* [Chebrolu et al \(2021\)](#).

Instead of applying an off-the-shelf robust estimator after learned descriptors, some works convert the entire pose estimation into the end-to-end training pipeline. Deep Closest Point (DCP) [Wang and Solomon \(2019\)](#) revises the original ICP pipeline

to a differentiable one that can learn from data. DeepGMR [Yuan et al \(2020\)](#) is the first learning-based method that leverages point-to-distribution correspondences for registration. Recently, the attention mechanism is also adopted to replace the role of feature matching and outlier filtering and thus can be used in end-to-end frameworks [Huang et al \(2021a\)](#); [Shi et al \(2021\)](#); [Yew and Lee \(2022\)](#). This data-driven works [Wang and Solomon \(2019\)](#); [Yuan et al \(2020\)](#); [Huang et al \(2021a\)](#); [Shi et al \(2021\)](#); [Yew and Lee \(2022\)](#) are trained and validated on public point cloud datasets. More data are necessary to ensure the robustness and generalization ability needed by global localization on mobile robotics.

3.2.2 Correspondence-free

The main idea of correspondence-free methods is to register point clouds based on feature similarity. With the convergence considered, existing methods can be divided into locally convergent and globally convergent methods. The locally convergent methods stem from the optical flow in the image domain. Instead of using 3D coordinates, PointNetLK [Aoki et al \(2019\)](#) uses PointNet [Qi et al \(2017\)](#) to learn the local feature of each point and then iteratively align the learned features. There also exist improved versions of PointNetLK framework [Li et al \(2021b\)](#); [Huang et al \(2020\)](#). One disadvantage of this class of approaches is the iterative solver, which is sensitive to initialization and may mislead the feature learning.

Globally convergent approaches are mainly based on the idea of correlation. Like the image registration pipeline, Bulow *et al.* [Bülow and Birk \(2018\)](#) utilize 3D Fourier-Mellin transform to achieve globally convergent 3D registration. PHASER [Bernreiter et al \(2021a\)](#) generates spherical frequency spectrum using Fourier transform and Laplace fusion and registers point cloud by calculating correlation. Zhu *et al.* [Zhu et al \(2022\)](#) propose to learn an embedding for each point cloud in a feature space that preserves the $SO(3)$ -equivariance property. The global convergence mostly contributed to the correlation, an inherently exhaustive search that can be evaluated effectively by spectrum decoupling.

Summary. Point cloud registration is a popular topic but there still remain some issues for mobile robotic applications, e.g., generalization ability under an end-to-end framework and alignment with less overlap. In certain applications, only local pose estimation can also provide global localization results, e.g., LiDAR LCD with ICP registration if the current pose is close to previous ones. If we combine approaches introduced in Section 3.1 and 3.2, a complete global localization framework can be obtained in a coarse-to-fine manner: *first global place recognition then followed by local pose estimation*.

Compared to place recognition-only approaches, the coarse-to-fine framework can provide precise poses for global localization tasks. The cost is that the map needs to include both global descriptors for retrieval and local metric points for state estimation. This makes the framework impracticable in large-scale environments, e.g., self-driving cars in city-scale environments for commercial use. Additionally, if place recognition fails, local pose estimation will suffer from this failure. We will introduce pose estimation-coupled place recognition to address these problems.

3.3 Pose Estimation-coupled Place Recognition

For the approaches explained in Section 3.2, two individual steps are needed to handle place recognition and local pose estimation. One upgrade direction is to design a shared feature embedding or representation that place recognition and pose estimation can benefit from it. Thus, *place recognition and local pose estimation could share the same processing pipeline*, making the map more concise and the state estimator tighter. We name this kind of approach pose estimation-coupled place recognition, or coupled methods for clearance.

Note that many methods in this section use the same pre-processing approaches in Section 3.1: *dense points/voxel-based, sparse segments-based and projection-based*. These methods can be classified based on the dimension of output poses, stated as follows.

3.3.1 3-DoF pose estimation

For mobile robots working on planar surfaces, pose estimation mainly focuses on three degrees of freedom (3-DoF): position and heading (yaw angle). One of the well-known methods is scan context Kim and Kim (2018). The 3D point clouds are divided into azimuthal and radial bins, in which the value is assigned to the maximum height of the points in it. The similarity is the sum of cosine distances between all the column vectors at the same indexes. As the column would shift when the viewpoint of the LiDAR changes, the authors propose a rotation-invariant descriptor extracted from scan context for top-k retrieval during place recognition, then further calculated the similarity and azimuth by column shift. The rotation here is the yaw angle or the heading for mobile robots moving on planar.

Some following methods are designed to improve the discriminability and invariance of the original scan context Wang et al (2020a); Li et al (2021a); Kim et al (2019); Wang et al (2020b); Xu et al (2021b). For example, Wang *et al.* Wang et al (2020a) utilize the maximum intensity within each bin as the descriptor. Li *et al.* Li et al (2021a) introduce the semantic labels of the point clouds. Researchers also extract deep learning-based features from scan context for better performance Kim et al (2019); Xu et al (2021b). Besides feature extraction, other methods improve the efficiency of the similarity calculation process by taking advantage of the circular cross-correlation property in scan context representation. Wang *et al.* Wang et al (2020b) utilized Fourier transform to estimate the translation shift along the azimuth-related axis. Xu *et al.* Xu et al (2021b) proposed a differentiable phase correlation method based on Fourier transform to make the place recognition and pose estimation (rotation) trained in an end-to-end manner.

Different from the scan context family that projects 3D point clouds into 2D polar bird’s-eye view (BEV) images, some methods transform point clouds into range images based on a spherical projection model. OREOS Schaupp et al (2019) utilizes a convolutional neural network to extract features on the range images and generates two vectors for place recognition and azimuth estimation simultaneously. OverlapNet Chen et al (2020a) estimates the overlap between two range images by calculating all possible differences for each pixel and calculating the azimuth taking advantage of the

circular cross-correlation. An improved version, OverlapTransformer [Ma et al \(2022b\)](#) is also proposed with a rotation-invariant representation and faster inference. The advantage of OverlapTransformer is the missing ability to provide yaw angle estimation. It is worth mentioning that the OverlapNet family uses the overlap of range images for loss function construction, which is different from the location-based loss in other learning-based methods, like contrastive loss in [Yin et al \(2017\)](#), triplet and quadruplet loss in [Uy and Lee \(2018\)](#).

Though many place recognition methods are rotation-invariant, they cannot achieve translation invariance due to the egocentric modeling process [Ding et al \(2022\)](#). And few of these methods are able to calculate the translation drift between the query and retrieved point clouds. To relieve these limitations, scan context [Kim and Kim \(2018\)](#) augments the query point cloud with root-shifted point clouds. And later in scan context++ [Kim et al \(2021\)](#), Kim *et al.* propose the Cartesian BEV-based descriptor for translation estimation. RING by Lu *et al.* [Lu et al \(2022\)](#) propose a non-egocentric Cartesian BEV-based descriptor with both rotational and translational invariance. Besides place recognition and azimuth estimation, translation can also be estimated with this unified descriptor.

3.3.2 6-DoF pose estimation

Many visual global localization frameworks extract local descriptors on images for both place recognition and the following pose estimation. Generally, the local features are aggregated into a global descriptor using methods such as bag-of-words (BoW) [Gálvez-López and Tardos \(2012\)](#), VLAD [Jégou et al \(2010\)](#), or ASMK [Tolias et al \(2013\)](#). Meanwhile, 6-DoF poses are often extracted from visual data from using Perspective-n-Point (PnP) algorithms [Lepetit et al \(2009\)](#) based on the matched local features. Inspired by visual image matching, some methods converted LiDAR point clouds into images and applied similar techniques to the transferred images. Shan *et al.* [Shan et al \(2021\)](#) utilize the traditional BoW algorithm in visual place recognition for LiDAR-based global localization. Specifically, they transform the intensity of the high-resolution lidar point cloud into images and extracted features based on Oriented FAST and rotated BRIEF (ORB) [Rubblee et al \(2011\)](#). The visual matching technique is also tested on [Di Giammarino et al \(2021\)](#). However, works by Shan *et al.* [Shan et al \(2021\)](#) and Giammarino *et al.* [Di Giammarino et al \(2021\)](#) require a high-resolution LiDAR scanner (64 and 128 rings) to guarantee the extraction and description of local features. In BVMatch [Luo et al \(2021\)](#), sparse LiDAR scans are first projected to BEV images and then visual matching techniques are applied. The cost is that the final pose is actually with 3-DoF [Luo et al \(2021\)](#).

Visual-inspired matching needs a projection to reduce the dimensionality of 3D point clouds. Some researchers propose to design discriminative 3D features for local matching and global descriptor encoding. It is becoming a new research trend in the last three years (2019-2022). DH3D by Du *et al.* [Du et al \(2020\)](#) uses flex convolution and squeeze-and-excitation block as the feature encoder and applies a saliency map for keypoint detection. Then the local features were aggregated into a global descriptor for place recognition. EgoNN by Komorowski *et al.* [Komorowski et al \(2021\)](#) transforms the point clouds into a cylindrical occupancy map, and develops a 3D convolutional

architecture based on MinkLoc3D [Komorowski \(2021\)](#) for keypoint regression and description. A structure-aware registration network is introduced in [Qiao et al \(2021\)](#) and it is trained in a virtual LiDAR dataset while tested in real-world environments. Cattaneo *et al.* [Cattaneo et al \(2022\)](#) propose an end-to-end LCDNet that can achieve both place recognition and pose estimation. LCDNet modifies PV-RCNN [Shi et al \(2020\)](#) for local feature extraction and builds a differentiable unbalanced optimal transport [Chizat et al \(2018\)](#) for feature matching. BoW3D [Cui et al \(2022a\)](#) utilizes 3D point cloud feature LinK3D [Cui et al \(2022b\)](#) for feature extraction and adapted BoW for global localization. Instead of point-level features, GOSMatch [Zhu et al \(2020\)](#) utilizes high-level semantic objects for global localization. The authors propose a histogram-based graph descriptor and vertex descriptor taking advantage of the spatial locations of semantic objects for place recognition and local feature matching. Similarly, BoxGraph [Pramatarov et al \(2022\)](#) encodes a semantic object and its shape of a 3D point cloud into a vertex of a fully-connected graph. The graph is used for both similarity measure and pose estimation. Yuan *et al.* [Yuan et al \(2022\)](#) propose a novel triangle-based global descriptor, stable triangle descriptor (STD) for place recognition and relative pose estimation. STD keeps a hash table as the global descriptor, and place recognition is achieved by voting of triangles in the table.

All the methods above achieve place recognition by nearest neighbor search or exhaustive comparisons on global descriptors. Several works only use local keypoints or features to build coupled methods, and there are no global descriptors for place retrieval. Bosse and Zlot [Bosse and Zlot \(2009, 2013\)](#) extract and describe keypoints for both place candidate voting and 6-DoF pose estimation. Inspired by the work of Bosse and Zlot [Bosse and Zlot \(2013\)](#), Guo *et al.* [Guo et al \(2019\)](#) design an intensity-integrated keypoint and also propose a probabilistic voting strategy. Steder *et al.* [Steder et al \(2010a\)](#) propose to match point features on range images and score potential transformations for final pose estimation. Instead of extracting features on point clouds, Millane *et al.* [Millane et al \(2019\)](#) introduce a SIFT-inspired [Lowe \(1999\)](#) local feature based on the distance function map of 2D LiDAR submaps. Experiments validate that using free space for submap matching performs better compared with using occupied grids.

Summary. Pose estimation-coupled place recognition outputs not only place retrievals but also a 3-DoF (or with only a 1-DoF yaw angle) or a full 6-DoF pose. Common evaluation metrics include both precision-recall for retrieval and quantitative errors compared to ground truth orientation or position.

One might ask about the advantages of using such methods compared to the previous two-step pipeline using place retrieval (Section 3.1) followed by precise pose estimation (Section 3.2). The potential advantages are three folds:

- **Lightweight map.** Dense point maps limit mobile robotic applications in large-scale environments, especially for resource-constrained vehicles. If place recognition and pose estimation share the same feature or representation, fewer data and sparser keyframes could support global localization in such conditions, making the entire map more lightweight to use.

- Geometric verification. For place recognition methods, a key issue is to verify whether a retrieved place is correct. Pose estimation results can be used as geometric verification to filter incorrect places. This filtering strategy has been applied in several coupled methods [Zhu et al \(2020\)](#); [Yuan et al \(2022\)](#).
- Initial guess for refinement. If an accurate pose is required, a local point cloud registration (Section 3.2) is necessary for pose refinement. Coupled approaches can provide an initial guess for such refine modules, thus improving the accuracy and efficiency of pose estimation. As reported in LCDNet [Cattaneo et al \(2022\)](#), the initial guess significantly reduces runtime and metric errors when applying ICP alignment.

Overall, the pose estimation and place recognition are coupled in this subsection, but keyframes or places are still needed in a pre-built map database. A one-stage global localization will be presented in the following subsection.

3.4 One-stage Global Pose Estimation

The two-stage methods using place recognition and pose estimation techniques have shown successful operations in various datasets and applications. Thus a natural question is raised: can we achieve global localization by directly matching on a global map without separating the map space? The answer is yes and some approaches can achieve one-stage global pose estimation. The majority of these approaches can be classified into two categories based on how to estimate the pose: in a traditional closed form or in an end-to-end manner.

3.4.1 Feature-based matching

One representative work is SegMatch proposed by Dubé *et al.* [Dubé et al \(2017\)](#) in 2017, with results illustrated in Figure 5. SegMatch first segments dense LiDAR map points to clusters with ground removal and then extracts features based on eigenvalues and shapes of segments. Random forest classifier is trained and applied to boost feature matching. Finally, matched candidates are fed into RANSAC for 6-DoF pose estimation. The handcrafted descriptors were extended to data-driven SegMap [Dubé et al \(2018\)](#) with the help of deep neural networks. In [Cramariuc et al \(2021\)](#), SemSegMap is proposed by integrating visual information into point cloud segmentation and feature extraction. SegMatch and its “family members” are validated and evaluated in urban and disaster environments.

Inspired by SegMatch scheme, Tinchev *et al.* [Tinchev et al \(2018\)](#) propose Natural Segmentation and Matching (NSM) for global localization in a more natural environment. The insight is a novel hybrid descriptor and is more robust to different points of view than the baseline SegMatch. Similarly, NSM has also been extended to a deep learning version in [Tinchev et al \(2019\)](#). In these feature-based global matching methods [Dubé et al \(2017, 2018\)](#); [Cramariuc et al \(2021\)](#); [Tinchev et al \(2018, 2019\)](#), point cloud segments are aligned with low-dimensional and distinctive descriptors for global matching. The global segment-based maps can support not only loop closing for consistent mapping but also pose tracking for online localization.

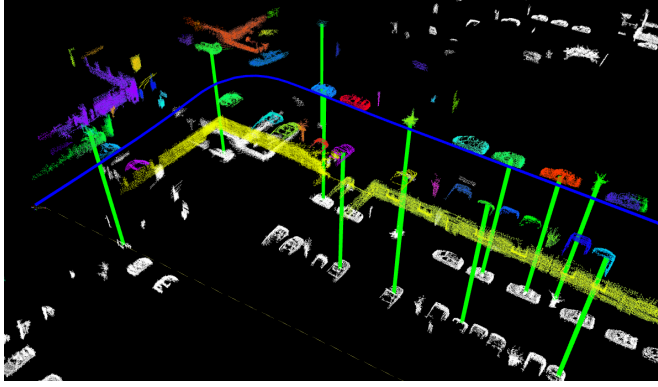


Fig. 5 From SegMatch [Dubé et al \(2017\)](#). SegMatch achieves global localization at the level of segments rather than conventional keypoints. Different colors represent the segmentation results. Segment matches are indicated with green lines.

Generally, these segmentation-based approaches rely on the point segmentation results, as mentioned in Section 3.1.2. A robot traveling is a good choice to accumulate dense 3D point clouds first, and then segmentation and segment matching are performed. Hence, these methods are less efficient compared to two-stage approaches in some specific tasks, like fast re-localization with sparse scans. In addition, the reliance on segments could make these methods fail in some challenging scenes, e.g., in a featureless flat field or a man-made environment with too many repetitive structures.

3.4.2 Deep regression

With the popularity of deep learning, several researchers propose to regress global robot pose directly in an end-to-end fashion, just like PoseNet [Kendall et al \(2015\)](#) for visual re-localization. Similarly, Wang *et al.* [Wang et al \(2021\)](#) propose a learning-based PointLoc for LiDAR global pose estimation. The backbone is an attention-aided PointNet-style architecture [Qi et al \(2017\)](#) for 6-DoF pose regression. This end-to-end manner is completely data-driven without conventional pose estimation processing. Lee *et al.* [Lee et al \(2022\)](#) convert the global localization as an unbalanced point registration problem, and propose a hierarchical framework UPPNet to solve this problem. Specifically, UPPNet first searches the potential subregion in a large point map and then achieves pose estimation via local feature matching in this subregion. UPPNet can also be trained in an end-to-end fashion.

Summary. Feature-based one-stage approaches do not use discrete places or locations for place recognition. They are suitable for loop closure detection in a small area, i.e., the solution space $|\mathbb{X}|$ is reduced to a smaller size in Equation 3. However, the downside is that it is challenging to re-localize a robot from scratch using partial local features in a large feature map.

As for one-stage deep regression approaches, though LiDAR scanner provides rich structural information, the metric estimation is not competitive [Wang et al \(2021\)](#); [Lee et al \(2022\)](#) compared to conventional two-stage methods in Section 3.2 and 3.3. We consider one-stage pose regression is a promising research direction in the era of

big data, but still remain many issues to solve, e.g., how to improve the interpretability and generalization ability of these end-to-end methods.

4 Global Localization using Sequential Measurements

Section 3 reviews related single-shot global localization approaches that take a single LiDAR point cloud as the input. As previously analyzed in Section 1.1, the map size $|\mathbf{M}|$ is generally much larger than the size of single point cloud $|\mathbf{z}_t|$, while the single-shot global localization methods can not guarantee the localization success in challenging scenes. On the other hand, LiDAR sensor provides high-frequency point measurements, and sequential point clouds can be obtained when the robot travels a distance. Thus taking multiple measurements $\mathbf{Z}_t \triangleq \{\mathbf{z}_{k=1}, \dots, \mathbf{z}_t\}$ could enhance the global localization performance choice with robot moving. This section reviews methods that use sequential LiDAR inputs for global pose estimation. Note that place retrieval methods in Section 3 can be integrated as a front-end matching in frameworks of this section.

Sequential global localization can be divided into two categories determined by its map and the use of place recognition and pose estimation. One is *sequential place matching* on keyframe-based submaps and the other is *sequential-metric global localization* on metric maps. The former provides a retrieved place as a localization result and is performed on keyframe-based submaps. The latter outputs an accurate pose on a metric map and is generally based on a global metric map.

As analyzed in Section 1.1, we consider that sequential-based approaches can also be classified into two categories: *batch processing* and *recursive filtering*. The difference is how to handle sequential information for global pose estimation: batch methods handle a batch of information to estimate the entire robot trajectory (Equation 4); filtering methods estimate the pose under Bayesian filtering or similar techniques (Equation 5). We will also talk about this taxonomy as an underlying theme in the following two subsections. We present several representative works in Table 2.

4.1 Sequential Place Matching

Probabilistic or sequential matching can help improve the visual localization success rate, which has been validated in several classical visual systems: FAB-MAP Cummins and Newman (2008), SeqSLAM Milford and Wyeth (2012); Milford et al (2015), the work of Naseer *et al.* Naseer et al (2018), and Vysotska and Stachniss Vysotska and Stachniss (2019). FAB-MAP first builds an appearance-based BoW for single image retrieval and then formulates recursive Bayesian filtering for global localization. An extended version FAB-MAP 3D Paul and Newman (2010) also models spatial information to improve the robustness of the framework. The filtering technique of FAB-MAP family could handle sequential measurements, but will easily crash when single-shot place recognition fails in challenging scenes. In SeqSLAM Milford and Wyeth (2012), a sequence-to-sequence matching strategy is proposed to find the location candidates in an image similarity matrix. SeqSLAM processes a batch of images compared to filtering-based methods, making the whole system more robust. The SeqSLAM family

Table 2 Representative Works of Sequential Global LiDAR Localization

Name	Pose	Learning	Handling	Backbone
Liu et al (2019a)	Place	Yes	Batch	LPDNet Liu et al (2019b) + Sequence Matching
Yin et al (2022b)	Place	Yes	Filter	SphereVLAD + Hierarchical Particle Filter
Ma et al (2022a)	Place	Yes	Batch	Multi-scan Transformer + GeM Pooling
Dellaert et al (1999)	3-DoF	No	Filter	Monte Carlo Localization (MCL)
Jonschkowski et al (2018)	3-DoF	Yes	Filter	Differentiable Particle Filter (Differentiable MCL)
Chen et al (2021a)	3-DoF	Yes	Filter	Deep Samplable Observation Model + Adaptive Mixture MCL
Gao et al (2019)	3-DoF	No	Filter	Feature Matching + Odometry + Multiple Hypothesis Tracking
Wang et al (2019)	6-DoF	No	Batch	Landmark Association + Odometry + Factor Graph

Batch: Batch Processing, Filter: Recursive Filtering

has demonstrated its success in both handcrafted features [Milford and Wyeth \(2012\)](#) and data-driven features [Milford et al \(2015\)](#). Naseer *et al.* [Naseer et al \(2018\)](#) propose to use a network flow to handle batch image matching and maintain multiple route hypotheses in parallel. Global visual matching method is also proposed in [Vysotska and Stachniss \(2019\)](#) for re-localization, in which the map database contains multiple sequences for graph-based search.

The LiDAR-based sequential matching has been inspired by visual methods in recent years. Liu *et al.* [Liu et al \(2019a\)](#) propose to use LPD-Net [Liu et al \(2019b\)](#) for front-end place recognition, and design a coarse-to-fine sequence matching strategy for global localization. The designed strategy improves the place retrieval performance compared with single-shot LPD-Net. Yin *et al.* [Yin et al \(2022b\)](#) present a particle-aided fast matching scheme in large-scale environments based on sequential place recognition results, which is generated by SphereVLAD in Section 3.1.3. From the viewpoint of state estimation, [Liu et al \(2019a\)](#) handles batch information while [Yin et al \(2022b\)](#) recursively estimates the locations. Recent work SeqOT [Ma et al \(2022a\)](#) generates one global descriptor for a sequence of range images, rather than multiple descriptors in its previous version [Ma et al \(2022b\)](#). Specifically, a novel end-to-end transformer is built to handle spatial and temporal information fusion.

All these methods above, visual- or LiDAR-based, aim at estimating the most likely (highest probability) match on topological keyframe-based submaps (Section 2.1). The evaluation of these methods is the same with place recognition-only approaches in Section 3.1.

4.2 Sequential-Metric Localization

If the map has a geometric representation, like occupancy grids and landmarks, it can enable metric pose estimation for mobile robots, making sequential global localization more practical.

Particle filter localization, also known as sequential Monte Carlo Localization (MCL) in the robotics community, is a widely used recursive state estimation back-end [Dellaert et al \(1999\)](#). Unlike the Kalman filters family, MCL is non-parametric Bayesian filtering without assuming the distributions of robot states. More specifically, it uses a group of samples to represent the robot state, which is naturally suitable for global localization tasks especially when the robot pose has a multi-modal distribution. Researchers have proposed multiple extended versions to improve the robustness and efficiency of the original MCL. Maintaining a large set of particles is computationally expensive. Adaptive MCL [Fox \(2001\)](#) is able to sample particles in an adaptive manner using the Kullback–Leibler divergence. In [Stachniss and Burgard \(2005\)](#), segmented patch maps are integrated into MCL framework, making it applicable in indoor non-static environments. Most LiDAR sensors can also intensity information as reflection properties of surfaces. [Bennewitz et al. Bennewitz et al \(2009\)](#) use these reflection properties to improve the observation model of MCL, and it achieves faster convergence for re-localization. Recent work [Zimmerman et al \(2022\)](#) also integrates human-readable text information into MCL for localization, making it more robust to structural changes in buildings. Due to its simplicity and effectiveness, MCL is also used in various low-dimensional navigation tasks beyond global localization, such as robotic pose tracking [Yin et al \(2022a\)](#) and exploration tasks [Stachniss et al \(2005\)](#).

Currently, MCL is one of the gold standards in multiple robot navigation toolkits [Montemerlo et al \(2003\)](#); [Zheng \(2021\)](#). Indoor LiDAR MCL is well studied and has been widely deployed for commercial use, e.g., applying to a home cleaning robot. A recent trend of indoor LiDAR localization is to use building architectures as maps, e.g., structural computer-aided design (CAD) [Boniardi et al \(2017\)](#); [Zimmerman et al \(2023\)](#) and semantic building information modeling (BIM) [Yin et al \(2023\)](#); [Hendriks et al \(2021\)](#). These maps are easy to obtain and keep sparse but critical information of environments, like walls and columns. The use of such maps makes the localization free of pre-mapping for long-term operations. MCL can also be used for localization on floor plan maps [Boniardi et al \(2017\)](#); [Zimmerman et al \(2023\)](#). Experiments show that such cheap maps can also support indoor robot localization.

Modern MCL methods integrate discrete place recognition techniques into the filtering framework, making MCL applicable in large-scale outdoor environments. [Yin et al. Yin et al \(2018\)](#) propose to use the Gaussian mixture model to fuse multiple place recognition results, and then integrate it into the MCL system as a measurement model. With the convergence of MCL, a coarse pose can be generated as an initial guess for accurate ICP refinement. The observability of orientation is also proofed in its extended version [Yin et al \(2019b\)](#). Similarly, [Chen et al. Chen et al \(2020b\)](#) use their OverlapNet [Chen et al \(2020a\)](#) to extract features of submaps in a global map and propose a new observation model for MCL by comparing the similarity between the current feature and the stored features to achieve global LiDAR localization. [Sun et al. Sun et al \(2020\)](#) and [Akai et al. Akai et al \(2020\)](#) propose to fuse deep pose

regression and MCL to build a hybrid global localization, in which deep pose regression could provide a 3-DoF or 6-DoF from an end-to-end neural network. The methods above [Yin et al \(2019b\)](#); [Chen et al \(2020a\)](#); [Sun et al \(2020\)](#); [Akai et al \(2020\)](#) typically discretize the pose and map space for fast convergence of MCL in large-scale environments. A deep learning-aided samplable observation model was proposed in [Chen et al \(2021a\)](#), named DSOM. Given a 2D laser scan and a global indoor map, DSOM can provide a probability distribution for MCL on the global map, thus making particle sampling focus on high-likelihood regions.

The advancements caused by deep learning methods also affect the back-end state estimator of the MCL system. Jonschkowski *et al.* [Jonschkowski et al \(2018\)](#) propose a differentiable particle filter (DPF) for robot pose tracking and global localization. The whole DPF pipeline includes differentiable motion and measurement models, and a belief update model for particles, making the DPF trainable in an end-to-end manner. In Differentiable SLAM-net proposed by Karkus *et al.* [Karkus et al \(2021\)](#), DPF was encoded into a trainable visual SLAM for indoor localization. LiDAR-based particle filter is quite mature and there is no LiDAR-based DPF currently. But we consider differentiable state estimator could be a promising direction in this era of big data.

We also notice that there exist other frameworks that can achieve sequential-metric global localization. Multiple hypotheses tracking (MHT) [Thrun \(2002\)](#) is a possible solution to the global localization problem. An improved MHT framework is proposed in [Gao et al \(2019\)](#), and authors design a new structural unit encoding scheme to weight hypotheses. Hendrikx *et al.* [Hendrikx et al \(2022\)](#) propose to build a hypotheses tree for indoor global localization. A global feature map is required for this method and explicit data associations are used to check the hypotheses. Wang *et al.* [Wang et al \(2019\)](#) provide a factor graph-based global localization from a floor plan map (GLFP). GLFP integrates odometry information and landmark matching into a factor graph when the robot travels. Compared to the filtering family (MCL and MHT), GLFP handles a batch of information for global pose estimation, which is similar with SeqSLAM in Section 4.1. The landmark matching actually provides global position information for factor graph optimization. In the works of Wilbers *et al.* [Wilbers et al \(2019\)](#), researchers employ graph-based sliding window approaches to fuse outdoor landmark matching and odometry information. Merfels and Stachniss *et al.* [Merfels and Stachniss \(2016\)](#) fuse global poses from GNSS and odometry information to achieve self-localization for autonomous driving. Lastly, in this subsection, the evaluation typically contains metric pose estimation on the map, e.g., using Root Mean Square Error (RMSE), which differs from approaches in Section 4.1.

5 LiDAR-aided Cross-Robot Localization

The review in Section 3 and Section 4 mainly focuses on single robot-based global LiDAR localization. Global localization can also be deployed into multi-robot systems for cross-robot localization, which is a new trend in the robotics community. More concretely, one robot performs mapping and another robot globally estimates its pose on this map, and vice versa.

Table 3 Representative Works of Cross-robot Localization

Name	Environment	Robot Team	Backbone and Highlight
Ebadi et al (2021)	Subterranean	Heterogeneous	LCD by Feature Matching + Degeneracy-aware LiDAR SLAM
Chang et al (2022)	Subterranean	Heterogeneous	LCD by GICP + Outlier-robust PGO
Huang et al (2021b)	Park	Wheeled	LCD by Scan Context Kim and Kim (2018) + PCM + PGO
Zhong et al (2022)	Campus	Wheeled	LCD by LiDAR Iris Wang et al (2020b) + PCM + PGO
Xu et al (2022b)	Campus	Legged	LCD by roto-invariant RING Lu et al (2022) + ICP + PGO

¹ PGO: Pose Graph Optimization, PCM: Pairwise Consistent Measurement Set Maximization

² Environment is the real robot platforms working in, not the dataset.

In practice, the multi-robot system is a broad topic that involves many subproblems that are not the main concerns of this paper, such as communication bandwidth and computation efficiency. As for system architecture, we mainly focus on *distributed* multi-robot systems, which is different *centralized* map servers [Bernreiter et al \(2022\)](#); [Cramariuc et al \(2022\)](#). We also note that customized scan matching is proposed for point cloud map fusion and collaborative robots [Yue et al \(2022\)](#). These localization methods are based on offline map appearance, while this section mainly focuses on incremental keyframe-based cross-robot localization. Several representative works are listed in Table 3.

Over the last two decades, there has been a growing demand for autonomous exploration and mapping of various environments, ranging from outdoor cluttered and underground environments to complex cave networks. Due to this, multi-robot SLAM, a critical solution for navigation in GNSS-denied areas where prior maps are unavailable, is receiving more attention. The recent DARPA Subterranean (SubT) Challenge, a three-year global competition that ended in 2021, aimed to demonstrate and advance the state-of-the-art in mapping, localization, and exploration of complex underground settings and has been particularly important in improving multi-robot SLAM. The multi-robot SLAM architectures adopted by the six SubT teams are summarized in the survey by Ebadi *et al.* [Ebadi et al \(2022\)](#). Although many loop closure methods were proposed then, most of the teams detected loop closure candidates simply by calculating the distance between the current keyframe and another keyframe in the factor graph. This LCD strategy is the same as DARE-SLAM [Ebadi et al \(2021\)](#) and LAMP [Chang et al \(2022\)](#); [Denniston et al \(2022\)](#). The simple but effective LCD used in these methods mainly relies on the setting that all robots start to move in the same starting region. In this context, with a high-precision LiDAR odometry [Zhang and Singh \(2014\)](#); [Zhao et al \(2021\)](#) at the front end, the distance-based LCD can work well in a relatively small (<5 km) area. There is no need to customize a complex place retrieval module in the robotic system [Ebadi et al \(2022\)](#).

Despite the underground exploration, robots might not always be able to begin a task at the same location, as in large-scale search and rescue tasks. As a result,

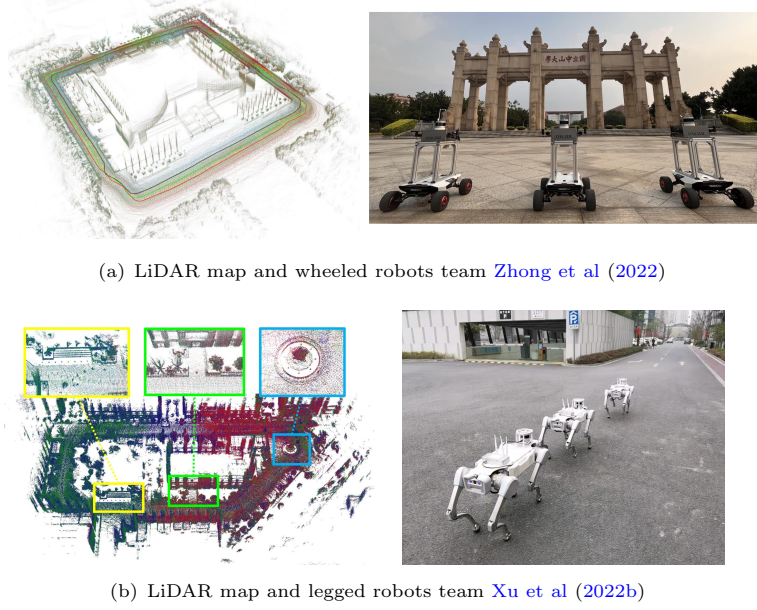


Fig. 6 Qualitative results from DCL SLAM [Zhong et al \(2022\)](#) and RING++ [Xu et al \(2022b\)](#). Different colors represent LiDAR maps and trajectories generated from different mobile robots: wheeled robots in DCL SLAM and legged robots in RING++.

place recognition that does not rely solely on initials is necessary. In an aerial-ground collaborative manner, He *et al.* [He et al \(2020\)](#) extract obstacle outlines from submap point clouds and generate thumbnail images. The thumbnail images are converted into compact place descriptors by applying NetVLAD [Arandjelovic et al \(2016\)](#). DiSCo-SLAM [Huang et al \(2021b\)](#) firstly adopts LiDAR-based global descriptor, scan context [Kim and Kim \(2018\)](#), to perform place recognition in a distributed manner. The lightweight scan context descriptor makes the real-time application possible, although there are no field experiments with multi-robots in this paper. RDC-SLAM [Xie et al \(2021\)](#) utilizes a place-recognition-only global descriptor, called DELIGHT [Cop et al \(2018\)](#), to reduce time consumption. In the relative pose estimation part, eigenvalue-based segment descriptors are proposed to achieve feature matching. DCL-SLAM [Zhong et al \(2022\)](#) assesses the performance of LiDAR-Iris [Wang et al \(2020c\)](#), M2DP [He et al \(2016\)](#) and scan context [Kim and Kim \(2018\)](#) and finally uses the effective and rotation-invariant LiDAR-Iris for loop closure detection. Unlike the system-oriented research mentioned above, RING++ [Xu et al \(2022b\)](#) presents a general non-learning framework to achieve roto-translation invariance with various local features while estimating the relative 3-DoF pose. The roto-translation invariant property and the robust pose estimator allow the multi-robot system to sample places along a long distance while being computationally and memory efficient. Figure 6 shows the real-world experimental results using DCL SLAM [Zhong et al \(2022\)](#) and RING++ [Xu et al \(2022b\)](#).

From the systems above [He et al \(2020\)](#); [Huang et al \(2021b\)](#); [Xie et al \(2021\)](#); [Zhong et al \(2022\)](#); [Xu et al \(2022b\)](#), it can be concluded that inter-robot LCD methods enable cross-robot localization in large-scale environments. However, no LiDAR LCD method can provide perfect loop closures without false positives. The false positives are outliers that make estimation systems unstable and inaccurate. More specifically, almost all cross-robot localization systems are built on graph optimization frameworks [Kümmerle et al \(2011\)](#); [Dellaert \(2012\)](#). These false positives provide inconsistent links between pose nodes. The optimization may not converge to a correct solution in such conditions. This problem exists not only in LiDAR-aided cross-localization but also in other SLAM-related problems with different sensors.

There exist mainly two ways to handle this problem: one is to design a robust kernel or function to filter outliers *during* the graph optimization; another is to build an outlier rejection module *before* the optimization or similar techniques. Both of these two kinds of methods aim at improving the robustness of graph optimization by removing inconsistent edges generated from LCD methods. For robust kernel functions, a commonly used one is the Huber function [Huber \(1973\)](#) but it can not reduce the effectiveness of outlier edges in graphs [Sünderhauf and Protzel \(2012\)](#). Sünderhauf and Protzel [Sünderhauf and Protzel \(2012\)](#) propose to formulate switchable constraints in the optimization. The added constraints follow different outlier rejection policies, and they can turn on or turn off loop closures. Then Agarwal *et al.* [Agarwal et al \(2013\)](#) introduce scaling factors to replace the switchable constraints. The improved version achieves a faster convergence while still keeping the robustness of graph optimization. An iterative approach RRR is proposed in [Latif et al \(2013\)](#) and it identifies true positives via clustering consistent loop closures. Robust kernels and functions [Sünderhauf and Protzel \(2012\)](#); [Agarwal et al \(2013\)](#); [Latif et al \(2013\)](#) are typically integrated into pose graph optimization frameworks [Kümmerle et al \(2011\)](#); [Dellaert \(2012\)](#).

Outlier rejection modules are independent of back-end estimators. RANSAC [Fischler and Bolles \(1981\)](#) is a popular method for outlier rejection, which iteratively estimates a model from sampled data (loop closures). RANSAC starts in a random way and it needs fine-tuned parameters to fit the model. Olson *et al.* [Olson et al \(2005\)](#) propose a graph theory-based outlier rejection method, named single-cluster graph partitioning (SCGP). Note that the graph is generated from the adjacency matrix of pose nodes and not the pose graph for SLAM. SCGP estimates a pairwise consistency set as the final result via clustering in this graph. SCGP shows competitive performance with RANSAC. Similarly, the outlier rejection is formulated as a maximum set estimation problem in the work by Carlone *et al.* [Carlone et al \(2014\)](#). In 2018, Enqvist *et al.* present a pairwise consistency maximization (PCM) [Mangelson et al \(2018\)](#) for consistent mapping with loop closures.

PCM is a graph theory-guided algorithm for outlier rejection. PCM first builds a binary consistency graph by checking all loop closures of each other. The criteria of consistency check are formulated based on the transformation from odometry modules and loop closures. After all the loop closures are checked, a consistency graph can be obtained and each edge denotes the consistency between a pair of loop closures. PCM aims at estimating the maximum pairwise internally consistent set, which is the maximum clique problem in graph theory (the same problem mentioned in TEASER [Yang](#)

et al (2021), see Section 3.2). A fast clique solver by Pattabiraman *et al.* Pattabiraman et al (2015) is adopted in PCM Mangelson et al (2018). There also exist other solutions for this NP-hard problem Lusk et al (2021). As tested in Mangelson et al (2018), PCM achieves better performance compared with other robust kernels or outlier rejection modules Fischler and Bolles (1981); Agarwal et al (2013); Olson et al (2005). PCM has been validated in aforementioned LiDAR-aided cross-robot localization systems Huang et al (2021b); Zhong et al (2022), and other robot localization and mapping systems in recent years Xu et al (2022a); Tian et al (2022).

In summary, cross-robot localization is becoming a promising direction for future study. It involves multiple topics of robotics, such as odometry, LCD and robust estimator. The cross-robot localization topic is closely related to crowd-sourced mapping Herb et al (2019) for self-driving cars, which involves other important topics that are beyond the scope of this survey.

6 Open Problems

We begin the discussion section with a question: which is the best global LiDAR localization method? We consider that it is decided by many key factors: environments, maps and required pose accuracy, etc. There is no single best method to handle all applications and scenarios. *Users need to customize the global localization system according to what they actually need.* However, several popular methods have been validated and integrated into LiDAR-aided navigation systems. For example, particle filter family Dellaert et al (1999) is widely used to handle 3-DoF re-localization for wheeled robots. For vehicle localization in urban environments, scan context family Kim and Kim (2018) could be a good choice for loop closure detection due to its simplicity and learning-free scheme. For local pose estimation in SLAM, we kindly take MULLS Pan et al (2021a) as an example. MULLS extracts feature points and uses TEASER Yang et al (2021) for global registration in its loop closure module.

Overall, modern global LiDAR localization techniques have enabled several important functionalities for mobile robots. However, there are still open problems and worthy topics for future study. We will discuss these problems and conclude several promising directions for global LiDAR localization.

6.1 Evaluation Difference

Experimental validation and evaluation are critical for research papers. We notice that related papers evaluate their methods with different metrics. We briefly categorize these metrics into two parts as follows.

- Based on place retrieval. Any place recognition methods evaluate the global localization performance under machine learning metrics, like Recall@1% Uy and Lee (2018), precision-recall curves Kong et al (2020) and localization probability Dubé et al (2017); Yin et al (2019b) etc. In this context, a robot is localized successfully if the retrieved place is close to the ground truth position ($< d$ m). The threshold d is a user-defined parameter and related to the resolution of topological keyframe-based submaps, like 25m in Uy and Lee (2018) and 3m in Kong et al (2020).

- Based on pose estimation. Conventional LiDAR SLAM and map-based localization evaluate the performance based on rotation and translation errors. These errors are obtained by comparing the estimated global pose with the ground truth pose quantitatively. Several global localization approaches follow these metrics [Kim et al \(2021\)](#); [Cattaneo et al \(2022\)](#).

From the metrics above, a natural question is raised: which is the primary evaluation metric for global lidar localization? Compared to other onboard sensors, LiDAR sensors provide precise and stable range measurements. More importantly, in a classical scheme of autonomous mobile robots [Siegwart et al \(2011\)](#), an accurate pose state is desired from downstream planning and control modules. Hence, we argue that *place retrieval is not the ultimate goal for the global LiDAR localization problem, and pose estimation metrics are more meaningful*. As presented in the previous review [Toft et al \(2020\)](#), visual localization methods are evaluated and discussed with 6-DoF poses. Currently, there is no lidar localization are evaluated in the same pose estimation metric like [Toft et al \(2020\)](#), and it could be a future direction for the study on global LiDAR localization. In addition to the pose accuracy, the time cost of global localization is also a critical evaluation for a real-world robot system.

6.2 Multiple Modalities

Modern mobile robots are equipped with multiple sensors for self-localization [Jiao et al \(2022\)](#). In recent years, multi-modal sensing has been a hot topic in the community and has attracted much research interest. Different modalities bring direct challenges for *cross-modality* global localization. But on the other hand, each sensor modality has its pros and cons, and sensor *modality fusion* can potentially improve the reliability and robustness of localization. Despite the sensor modalities at the front end, recent learning techniques enable modality study to higher-level tasks, and we will also introduce *high-level semantics* in the LiDAR global localization problem.

Cross Modality. When offline mapping and online localization use different sensor modalities, we name it cross-modality localization. [Cattaneo et al. \(2020\)](#) propose to train 2D images and 3D point place recognition together. To achieve this, a deep neural network is built, integrating classical 2D convolution layers and 3D PointNet. Similarly, in [Yin et al \(2021\)](#), radar and LiDAR are mixed together for BEV-based place recognition. Overhead satellite imagery is a cheap source for outdoor localization that does not require lidar mapping beforehand. Metric global LiDAR localization on 2D satellite imagery is proposed and validated in [Tang et al \(2021\)](#). OpenStreetMap (OSM) is also an alternative map that includes structural road and building information. In [Cho et al \(2022\)](#), LiDAR descriptors are matched to OSM descriptors to achieve place recognition. For metric localization, a 4-bit representation is proposed in [Yan et al \(2019\)](#) that can measure the hamming distance between laser scans and OSM. Then the distances are used to formulate the observation model of MCL. Overall, the research insight of these works [Cattaneo et al \(2020\)](#); [Yin et al \(2021\)](#); [Tang et al \(2021\)](#); [Cho et al \(2022\)](#); [Yan et al \(2019\)](#) is to build a shared low-dimensional representation that can connect different data modalities. Precise and

global cross-modality global localization is still a challenging problem, e.g., matching a 2D visual image on a 3D LiDAR map.

Modality Fusion. Another direction is to build sensor fusion modules based on multiple modalities. A LiDAR-Vision segment descriptor achieves better performance for place recognition tasks than a LiDAR-only descriptor, as validated in [Ratz et al \(2020\)](#). Inspired by this, Coral [Pan et al \(2021b\)](#) designs a bi-modal place recognition by fusing colorful visual features and structural LiDAR elevation maps. AdaFusion [Lai et al \(2022\)](#) uses an attention scheme to weight visual and LiDAR modalities for place recognition. In [Bernreiter et al \(2021b\)](#), a spherical projection enables the fusion of visual and LiDAR at the front end without losing information. From these works above [Ratz et al \(2020\)](#); [Pan et al \(2021b\)](#); [Lai et al \(2022\)](#); [Bernreiter et al \(2021b\)](#), we can conclude that modality fusion can help improve the place recognition performance, but extra learning techniques are needed to fuse different modalities.

High-level Semantics As mentioned in Section 3.1, raw LiDAR point clouds are textureless and in an irregular format compared to visual images. This constrains high-level robotics applications, such as scene understanding and moving object detection. Behley *et al.* [Behley et al \(2021\)](#) released a large semantic LiDAR dataset in 2019, named SemanticKITTI. SemanticKITTI contains point-wise annotated LiDAR scans, and multiple semantic-related benchmarks for on-road autonomous navigation. A backbone network RangeNet++ [Milioto et al \(2019\)](#) and a semantic LiDAR SLAM SuMa++ [Chen et al \(2019\)](#) are also released publicly trained on semantic information provided by SemanticKITTI. The SemanticKITTI focuses on on-road robotic perception tasks, and we also note that there exists an off-road semantic LiDAR dataset, named RELIS-3D [Jiang et al \(2021\)](#). RELIS-3D also provides a full stack of multi-modal sensor data for field robotics research. The semantic information of LiDAR benefits both place recognition and pose estimation for global localization. In [Kong et al \(2020\)](#); [Vidanapathirana et al \(2021\)](#); [Pramatarov et al \(2022\)](#), semantics are used to construct a semantic-spatial graph for global descriptor extraction. It is validated that using semantic information can improve place recognition performance under this graph representation. Beyond the semantic representations, semantic-aided ICP is formulated for LiDAR odometry [Chen et al \(2019\)](#) and global point cloud alignment [Li et al \(2021a\)](#).

6.3 Less Overlap

Though the LiDAR scanner is powerful for environmental sensing, there exists a potential challenge when applying global LiDAR localization in practice: the overlap between two LiDAR point clouds might be very small in certain cases. For the global localization problem, the point clouds could be two scans or submaps for place retrieval, or scan-to-submap registration for pose estimation. Less overlap will make global localization techniques much more difficult. To better understand this challenge, we list three typical cases as follows.

Occlusions by dynamics. LiDAR scans will be partially blocked by dynamics in a high-dynamical environment, like pedestrians and vehicles around the robot. More specifically, for a spinning LiDAR sensor, the block area is decided by mainly two factors: the distance between dynamics and sensor, and the size of this dynamic. By far,

dynamics removal in LiDAR scans effectively and efficiently is still quite difficult [Lim et al \(2021\)](#). Compared to 360-degree rotating lidar sensors, some other range sensors can provide range data that are not easily blocked, like limited FoV solid LiDAR sensor [Yuan et al \(2022\)](#), imaging radar [Kramer et al \(2022\)](#), and spinning radar [Kim et al \(2020\)](#).

Large translation. For sparse keyframe-based submaps, a large translation between the retrieved keyframe and ground truth pose could result in a small overlap between the current LiDAR scan and the submaps stored in the keyframe. A powerful global point cloud registration is required to overcome this challenge.

Viewpoint change. Generally, for wheeled robots on roads, pose estimation is constrained in a 3-DoF space (x, y and yaw). But for flying drones in the wild, it is a complete 6-DoF pose estimation problem. When using global LiDAR localization on drones, LiDAR point clouds collected by drones might have less overlap at the same place. This is mainly due to two reasons: the 6-DoF motions of drones and the limited field-of-view (FoV) of LiDAR sensors.

6.4 Generalization Ability

For learning-free methods, less parameter tuning is desired to ensure the generalization to new environments [Vizzo et al \(2022\)](#). As for learning-based methods, generalization ability is a big challenge that has to face, especially when there is less training to support these data-driven methods. We mainly list four basic problems when deploying existing global localization methods.

Sensor configuration. Currently, there are dozens of LiDAR types, and each type has its unique sensor parameters. The generalization from one LiDAR sensor to another could be a problem, e.g., training on Velodyne HDL-64E scans while testing on Ouster OS1-128 scans. Another potential problem is the displacement of LiDAR sensors. If roll or pitch angle changes, laser point density and distribution will change respectively, resulting in global localization failure even using state-of-the-art methods. However, if the global localization is conducted on accumulated submaps, sensor configuration could be a minor problem.

Unbalanced matching. Currently, most global LiDAR localization methods are tested using relatively good data quality. In other words, the input point cloud and point cloud map have similar point density and point cloud scale. However, when aligning one LiDAR scan to one larger submap, there exist deviations between these unbalanced two data. Unbalanced point matching [Lee et al \(2022\)](#) is still hard to solve since local features are quite different [Chang et al \(2021\)](#) in such conditions. Additionally, LiDAR sensors will be affected in challenging conditions, like rainy and snowy days [Pitropov et al \(2021\)](#) and even strong lights on roads [Carballo et al \(2020\)](#), which brings potential hazards for global LiDAR localization.

Unseen environments. The generalization in the unseen scenario is an old but still hard problem in the learning community. Cross-city and Cross-environments generalization remains underexposed for global LiDAR localization methods. For instance, Knights *et al.* [Knights et al \(2022b\)](#) release a challenging dataset Wild-Places for LiDAR place recognition in natural environments. There is a performance drop for advanced methods [Kim and Kim \(2018\)](#); [Xu et al \(2021a\)](#); [Komorowski](#)

(2022) compared to tests in urban environments. It could be concluded that there is a domain gap between structural urban environments and unstructured natural environments. To enable continuous learning in new scenes, incremental learning [Li and Hoiem \(2017\)](#) is a good choice that does not require retraining from scratch. Recent work InCloud [Knights et al \(2022a\)](#) achieves incremental learning for point cloud place recognition and it overcomes catastrophic forgetting caused by learning in new domains.

Trigger of global localization. In a complete localization system, pose tracking takes most of the computation while global localization is only activated when it is needed. Thus, a natural question is raised: when to trigger global localization? For LCD and cross-robot localization, the trigger of global localization could be one or multiple pre-defined criteria, like similarity threshold of descriptors or an adaptive distance in [Denniston et al \(2022\)](#). As for re-localization applications, a robot might believe it knows where it is while it does, and it is actually the classic kidnapped robot problem in [Thrun \(2002\)](#). In this context, detected localization failure could be a trigger condition for global re-localization. The LiDAR localization failure detection problem is identical to the point cloud alignment quality evaluation at the front end. Researchers propose to design multiple metrics and train classifiers to learn how to score this alignment quality [Yin et al \(2019a\)](#); [Adolfsson et al \(2022\)](#). While at the back-end, features of state estimator can be used for failure detection [Fujii et al \(2015\)](#). Localization failure prediction and avoidance is also a worthwhile studied topic for long-term autonomy [Nobili et al \(2018\)](#).

7 Conclusion

In this survey, we started with the problem formulation of global localization and list three typical situations: loop closure detection, re-localization, and cross-robot localization. Before reviewing concrete methods, we introduce basic maps for this problem. We then review single-shot approaches considering the cooperation of place recognition (place retrieval) and pose estimation (geometric transformation estimation). After that, sequential global localization and cross-robot localization are reviewed. Finally, we discuss challenging tasks and promising directions for future study.

Acknowledgment

We would like to thank Dr. Xiaqing Ding for her constructive suggestions.

References

- Adolfsson D, Castellano-Quero M, Magnusson M, et al (2022) Coral: Introspection for robust radar and lidar perception in diverse environments using differential entropy. *Robot Auton Syst* p 104136
- Agarwal P, Tipaldi GD, Spinello L, et al (2013) Robust map optimization using dynamic covariance scaling. In: *Proc. IEEE Int. Conf. Robot. Autom.*, pp 62–69

- Akai N, Hirayama T, Murase H (2020) Hybrid localization using model-and learning-based methods: Fusion of monte carlo and e2e localizations via importance sampling. In: Proc. IEEE Int. Conf. Robot. Autom., pp 6469–6475
- Aoki Y, Goforth H, Srivatsan RA, et al (2019) Pointnetlk: Robust & efficient point cloud registration using pointnet. In: Proc. IEEE Conf. Comput. Vis. Pattern Recognit., pp 7163–7172
- Arandjelovic R, Gronat P, Torii A, et al (2016) Netvlad: Cnn architecture for weakly supervised place recognition. In: Proc. IEEE Conf. Comput. Vis. Pattern Recognit., pp 5297–5307
- Arun KS, Huang TS, Blostein SD (1987) Least-squares fitting of two 3-d point sets. IEEE Trans Pattern Anal Mach Intell (5):698–700
- Bai X, Luo Z, Zhou L, et al (2020) D3feat: Joint learning of dense detection and description of 3d local features. In: Proc. IEEE Conf. Comput. Vis. Pattern Recognit., pp 6359–6367
- Bai X, Luo Z, Zhou L, et al (2021) Pointdsc: Robust point cloud registration using deep spatial consistency. In: Proc. IEEE Conf. Comput. Vis. Pattern Recognit., pp 15859–15869
- Barfoot TD (2017) State estimation for robotics. Cambridge University Press
- Barron JT (2019) A general and adaptive robust loss function. In: Proc. IEEE Conf. Comput. Vis. Pattern Recognit., pp 4331–4339
- Behley J, Garbade M, Milioto A, et al (2021) Towards 3d lidar-based semantic scene understanding of 3d point cloud sequences: The semantickitti dataset. Int J Robot Res 40(8-9):959–967
- Bennewitz M, Stachniss C, Behnke S, et al (2009) Utilizing reflection properties of surfaces to improve mobile robot localization. In: Proc. IEEE Int. Conf. Robot. Autom., pp 4287–4292
- Bernreiter L, Ott L, Nieto J, et al (2021a) Phaser: A robust and correspondence-free global pointcloud registration. IEEE Robot Autom Lett 6(2):855–862
- Bernreiter L, Ott L, Nieto J, et al (2021b) Spherical multi-modal place recognition for heterogeneous sensor systems. In: Proc. IEEE Int. Conf. Robot. Autom., pp 1743–1750
- Bernreiter L, Khattak S, Ott L, et al (2022) Collaborative robot mapping using spectral graph analysis. arXiv preprint arXiv:220300308
- Besl PJ, McKay ND (1992) Method for registration of 3-d shapes. In: Sensor fusion IV: control paradigms and data structures, Spie, pp 586–606

- Biber P, Straßer W (2003) The normal distributions transform: A new approach to laser scan matching. In: Proc. IEEE/RSJ Int. Conf. Intell. Robots Syst., pp 2743–2748
- Boniardi F, Caselitz T, Kümmerle R, et al (2017) Robust lidar-based localization in architectural floor plans. In: Proc. IEEE/RSJ Int. Conf. Intell. Robots Syst., pp 3318–3324
- Bosse M, Zlot R (2009) Keypoint design and evaluation for place recognition in 2d lidar maps. *Robotics and Autonomous Systems* 57(12):1211–1224
- Bosse M, Zlot R (2013) Place recognition using keypoint voting in large 3d lidar datasets. In: Proc. IEEE Int. Conf. Robot. Autom., pp 2677–2684
- Buehler M, Iagnemma K, Singh S (2009) The DARPA urban challenge: autonomous vehicles in city traffic, vol 56. Springer
- Bülöw H, Birk A (2018) Scale-free registrations in 3d: 7 degrees of freedom with fourier mellin soft transforms. *Int J Comput Vis* 126(7):731–750
- Cadena C, Carlone L, Carrillo H, et al (2016) Past, present, and future of simultaneous localization and mapping: Toward the robust-perception age. *IEEE Trans Robot* 32(6):1309–1332
- Cao S, Lu X, Shen S (2022) Gvins: Tightly coupled gnss–visual–inertial fusion for smooth and consistent state estimation. *IEEE Trans Robot*
- Carballo A, Lambert J, Monroy A, et al (2020) Libre: The multiple 3d lidar dataset. In: Proc. IEEE Intell. Veh. Symp., IEEE, pp 1094–1101
- Carlone L, Censi A, Dellaert F (2014) Selecting good measurements via l1 relaxation: A convex approach for robust estimation over graphs. In: Proc. IEEE/RSJ Int. Conf. Intell. Robots Syst., pp 2667–2674
- Cattaneo D, Vaghi M, Fontana S, et al (2020) Global visual localization in lidar-maps through shared 2d-3d embedding space. In: Proc. IEEE Int. Conf. Robot. Autom., pp 4365–4371
- Cattaneo D, Vaghi M, Valada A (2022) Lcdnet: Deep loop closure detection and point cloud registration for lidar slam. *IEEE Trans Robot*
- Chang MF, Dong W, Mangelson J, et al (2021) Map compressibility assessment for lidar registration. In: Proc. IEEE/RSJ Int. Conf. Intell. Robots Syst., pp 5560–5567
- Chang Y, Ebadi K, Denniston CE, et al (2022) Lamp 2.0: A robust multi-robot slam system for operation in challenging large-scale underground environments. *arXiv preprint arXiv:220513135*

- Chebrolu N, Labe T, Vysotska O, et al (2021) Adaptive robust kernels for non-linear least squares problems. *IEEE Robot Autom Lett* 6(2):2240–2247
- Chen R, Yin H, Jiao Y, et al (2021a) Deep samplable observation model for global localization and kidnapping. *IEEE Robot Autom Lett* 6(2):2296–2303
- Chen X, Milioto A, Palazzolo E, et al (2019) SuMa++: Efficient LiDAR-based Semantic SLAM. In: *Proc. IEEE/RSJ Int. Conf. Intell. Robots Syst.*
- Chen X, Labe T, Milioto A, et al (2020a) Overlapnet: Loop closing for lidar-based slam. In: *Proc. Robot., Sci. Syst. Conf.*
- Chen X, Labe T, Nardi L, et al (2020b) Learning an Overlap-based Observation Model for 3D LiDAR Localization. In: *Proc. IEEE/RSJ Int. Conf. Intell. Robots Syst.*
- Chen X, Vizzo I, Labe T, et al (2021b) Range Image-based LiDAR Localization for Autonomous Vehicles. In: *Proc. IEEE Int. Conf. Robot. Autom.*
- Chizat L, Peyre G, Schmitzer B, et al (2018) Scaling algorithms for unbalanced optimal transport problems. *Mathematics of Computation* 87(314):2563–2609
- Cho Y, Kim G, Lee S, et al (2022) Openstreetmap-based lidar global localization in urban environment without a prior lidar map. *IEEE Robot Autom Lett* 7(2):4999–5006
- Choy C, Park J, Koltun V (2019) Fully convolutional geometric features. In: *Proc. IEEE Conf. Comput. Vis. Pattern Recognit.*, pp 8958–8966
- Choy C, Dong W, Koltun V (2020) Deep global registration. In: *Proc. IEEE Conf. Comput. Vis. Pattern Recognit.*, pp 2514–2523
- Cohen TS, Geiger M, Kohler J, et al (2018) Spherical cnns. *arXiv preprint arXiv:180110130*
- Cop KP, Borges PV, Dube R (2018) Delight: An efficient descriptor for global localisation using lidar intensities. In: *Proc. IEEE Int. Conf. Robot. Autom.*, pp 3653–3660
- Cramariuc A, Tschopp F, Alatur N, et al (2021) Semsegmap–3d segment-based semantic localization. In: *Proc. IEEE/RSJ Int. Conf. Intell. Robots Syst.*, pp 1183–1190
- Cramariuc A, Bernreiter L, Tschopp F, et al (2022) maplab 2.0—a modular and multi-modal mapping framework. *IEEE Robot Autom Lett*
- Cui Y, Chen X, Zhang Y, et al (2022a) Bow3d: Bag of words for real-time loop closing in 3d lidar slam. *IEEE Robot Autom Lett*

- Cui Y, Zhang Y, Dong J, et al (2022b) Link3d: Linear keypoints representation for 3d lidar point cloud. arXiv preprint arXiv:220605927
- Cummins M, Newman P (2008) Fab-map: Probabilistic localization and mapping in the space of appearance. *Int J Robot Res* 27(6):647–665
- Dellaert F (2012) Factor graphs and gtsam: A hands-on introduction. Tech. rep., Georgia Institute of Technology
- Dellaert F, Fox D, Burgard W, et al (1999) Monte carlo localization for mobile robots. In: *Proc. IEEE Int. Conf. Robot. Autom.*, pp 1322–1328
- Deng H, Birdal T, Ilic S (2018) Ppfnet: Global context aware local features for robust 3d point matching. In: *Proc. IEEE Conf. Comput. Vis. Pattern Recognit.*, pp 195–205
- Denniston CE, Chang Y, Reinke A, et al (2022) Loop closure prioritization for efficient and scalable multi-robot slam. arXiv preprint arXiv:220512402
- Di Giammarino L, Aloise I, Stachniss C, et al (2021) Visual place recognition using lidar intensity information. In: *Proc. IEEE/RSJ Int. Conf. Intell. Robots Syst.*, pp 4382–4389
- Ding X, Xu X, Lu S, et al (2022) Translation invariant global estimation of heading angle using sinogram of lidar point cloud. In: *Proc. IEEE Int. Conf. Robot. Autom.*, pp 2207–2214, <https://doi.org/10.1109/ICRA46639.2022.9811750>
- Du J, Wang R, Cremers D (2020) Dh3d: Deep hierarchical 3d descriptors for robust large-scale 6dof relocalization. In: *Proc. Eur. Conf. Comput. Vis.*, Glasgow, UK
- Dubé R, Dugas D, Stumm E, et al (2017) Segmatch: Segment based place recognition in 3d point clouds. In: *Proc. IEEE Int. Conf. Robot. Autom.*, pp 5266–5272
- Dubé R, Cramariuc A, Dugas D, et al (2018) Segmap: 3d segment mapping using data-driven descriptors. arXiv preprint arXiv:180409557
- Dube R, Cramariuc A, Dugas D, et al (2020) Segmap: Segment-based mapping and localization using data-driven descriptors. *Int J Robot Res* 39(2-3):339–355
- Ebadi K, Palieri M, Wood S, et al (2021) Dare-slam: Degeneracy-aware and resilient loop closing in perceptually-degraded environments. *Journal of Intelligent & Robotic Systems* 102(1):1–25
- Ebadi K, Bernreiter L, Biggie H, et al (2022) Present and future of slam in extreme underground environments. arXiv preprint arXiv:220801787
- Elhousni M, Huang X (2020) A survey on 3d lidar localization for autonomous vehicles. In: *Proc. IEEE Intell. Veh. Symp.*, IEEE, pp 1879–1884

- Eppstein D, Löffler M, Strash D (2010) Listing all maximal cliques in sparse graphs in near-optimal time. In: International Symposium on Algorithms and Computation, Springer, pp 403–414
- Fan Y, He Y, Tan UX (2020) Seed: A segmentation-based egocentric 3d point cloud descriptor for loop closure detection. In: Proc. IEEE/RSJ Int. Conf. Intell. Robots Syst., pp 5158–5163
- Fischler MA, Bolles RC (1981) Random sample consensus: a paradigm for model fitting with applications to image analysis and automated cartography. *Communications of the ACM* 24(6):381–395
- Fox D (2001) Kld-sampling: Adaptive particle filters. *Proc Adv Neural Inf Process Syst* 14
- Freund Y, Schapire RE (1997) A decision-theoretic generalization of on-line learning and an application to boosting. *Journal of computer and system sciences* 55(1):119–139
- Fujii A, Tanaka M, Yabushita H, et al (2015) Detection of localization failure using logistic regression. In: Proc. IEEE/RSJ Int. Conf. Intell. Robots Syst., pp 4313–4318
- Gálvez-López D, Tardos JD (2012) Bags of binary words for fast place recognition in image sequences. *IEEE Trans Robot* 28(5):1188–1197
- Gao H, Zhang X, Yuan J, et al (2019) A novel global localization approach based on structural unit encoding and multiple hypothesis tracking. *IEEE Trans Instrum Meas* 68(11):4427–4442
- Garg S, Fischer T, Milford M (2021) Where is your place, visual place recognition? arXiv preprint arXiv:210306443
- Gong Y, Sun F, Yuan J, et al (2021) A two-level framework for place recognition with 3d lidar based on spatial relation graph. *Pattern Recognition* 120:108171
- Granström K, Callmer J, Ramos F, et al (2009) Learning to detect loop closure from range data. In: Proc. IEEE Int. Conf. Robot. Autom., pp 15–22
- Granström K, Schön TB, Nieto JJ, et al (2011) Learning to close loops from range data. *Int J Robot Res* 30(14):1728–1754
- Guivant JE, Nebot EM (2001) Optimization of the simultaneous localization and map-building algorithm for real-time implementation. *IEEE Trans Robot Autom* 17(3):242–257
- Guo J, Borges PV, Park C, et al (2019) Local descriptor for robust place recognition using lidar intensity. *IEEE Robot Autom Lett* 4(2):1470–1477

- Guo Y, Bennamoun M, Sohel F, et al (2016) A comprehensive performance evaluation of 3d local feature descriptors. *Int J Comput Vis* 116(1):66–89
- Hadsell R, Chopra S, LeCun Y (2006) Dimensionality reduction by learning an invariant mapping. In: 2006 IEEE Computer Society Conference on Computer Vision and Pattern Recognition (CVPR’06), pp 1735–1742
- He J, Zhou Y, Huang L, et al (2020) Ground and aerial collaborative mapping in urban environments. *IEEE Robot Autom Lett* 6(1):95–102
- He L, Wang X, Zhang H (2016) M2dp: A novel 3d point cloud descriptor and its application in loop closure detection. In: *Proc. IEEE/RSJ Int. Conf. Intell. Robots Syst.*, pp 231–237
- Hendrikx R, Pauwels P, Torta E, et al (2021) Connecting semantic building information models and robotics: An application to 2d lidar-based localization. In: *Proc. IEEE Int. Conf. Robot. Autom.*, pp 11654–11660
- Hendrikx R, Bruyninckx H, Elfring J, et al (2022) Local-to-global hypotheses for robust robot localization. *Frontiers in Robotics and AI* p 171
- Herb M, Weiherer T, Navab N, et al (2019) Crowd-sourced semantic edge mapping for autonomous vehicles. In: *Proc. IEEE/RSJ Int. Conf. Intell. Robots Syst.*, pp 7047–7053
- Hess W, Kohler D, Rapp H, et al (2016) Real-time loop closure in 2d lidar slam. In: *Proc. IEEE Int. Conf. Robot. Autom.*, pp 1271–1278
- Horn BK (1987) Closed-form solution of absolute orientation using unit quaternions. *Josa a* 4(4):629–642
- Huang S, Gojcic Z, Usvyatsov M, et al (2021a) Predator: Registration of 3d point clouds with low overlap. In: 2021 IEEE/CVF Conference on Computer Vision and Pattern Recognition (CVPR), pp 4265–4274, <https://doi.org/10.1109/CVPR46437.2021.00425>
- Huang X, Mei G, Zhang J (2020) Feature-metric registration: A fast semi-supervised approach for robust point cloud registration without correspondences. In: *Proc. IEEE Conf. Comput. Vis. Pattern Recognit.*, pp 11366–11374
- Huang Y, Shan T, Chen F, et al (2021b) Disco-slam: Distributed scan context-enabled multi-robot lidar slam with two-stage global-local graph optimization. *IEEE Robot Autom Lett* 7(2):1150–1157
- Huber PJ (1973) Robust regression: asymptotics, conjectures and monte carlo. *The annals of statistics* pp 799–821

- Hui L, Yang H, Cheng M, et al (2021) Pyramid point cloud transformer for large-scale place recognition. In: Proc. IEEE Conf. Comput. Vis. Pattern Recognit., pp 6098–6107
- Ito S, Endres F, Kuderer M, et al (2014) W-rgb-d: floor-plan-based indoor global localization using a depth camera and wifi. In: Proc. IEEE Int. Conf. Robot. Autom., pp 417–422
- Jiang P, Osteen P, Wigness M, et al (2021) Rellis-3d dataset: Data, benchmarks and analysis. In: Proc. IEEE Int. Conf. Robot. Autom., pp 1110–1116
- Jiao J, Wei H, Hu T, et al (2022) Fusionportable: A multi-sensor campus-scene dataset for evaluation of localization and mapping accuracy on diverse platforms. arXiv preprint arXiv:220811865
- Jonschkowski R, Rastogi D, Brock O (2018) Differentiable particle filters: End-to-end learning with algorithmic priors. arXiv preprint arXiv:180511122
- Jégou H, Douze M, Schmid C, et al (2010) Aggregating local descriptors into a compact image representation. In: 2010 IEEE Computer Society Conference on Computer Vision and Pattern Recognition, pp 3304–3311, <https://doi.org/10.1109/CVPR.2010.5540039>
- Kallasi F, Rizzini DL, Caselli S (2016) Fast keypoint features from laser scanner for robot localization and mapping. IEEE Robot Autom Lett 1(1):176–183
- Karkus P, Cai S, Hsu D (2021) Differentiable slam-net: Learning particle slam for visual navigation. In: Proc. IEEE Conf. Comput. Vis. Pattern Recognit., pp 2815–2825
- Kendall A, Grimes M, Cipolla R (2015) PoseNet: A convolutional network for real-time 6-dof camera relocalization. In: Proc. IEEE Int. Conf. Comput. Vis., pp 2938–2946
- Kim G, Kim A (2018) Scan context: Egocentric spatial descriptor for place recognition within 3d point cloud map. In: Proc. IEEE/RSJ Int. Conf. Intell. Robots Syst., pp 4802–4809
- Kim G, Park B, Kim A (2019) 1-day learning, 1-year localization: Long-term lidar localization using scan context image. IEEE Robot Autom Lett 4(2):1948–1955. <https://doi.org/10.1109/LRA.2019.2897340>
- Kim G, Park YS, Cho Y, et al (2020) Mulran: Multimodal range dataset for urban place recognition. In: Proc. IEEE Int. Conf. Robot. Autom., pp 6246–6253
- Kim G, Choi S, Kim A (2021) Scan context++: Structural place recognition robust to rotation and lateral variations in urban environments. IEEE Trans Robot

- Knights J, Moghadam P, Ramezani M, et al (2022a) Incloud: Incremental learning for point cloud place recognition. arXiv preprint arXiv:220300807
- Knights J, Vidanapathirana K, Ramezani M, et al (2022b) Wild-places: A large-scale dataset for lidar place recognition in unstructured natural environments. arXiv preprint arXiv:221112732
- Komorowski J (2021) Minkloc3d: Point cloud based large-scale place recognition. In: Proceedings of the IEEE/CVF Winter Conference on Applications of Computer Vision, pp 1790–1799
- Komorowski J (2022) Improving point cloud based place recognition with ranking-based loss and large batch training. arXiv preprint arXiv:220300972
- Komorowski J, Wysoczanska M, Trzcinski T (2021) Egonn: Egocentric neural network for point cloud based 6dof relocalization at the city scale. *IEEE Robot Autom Lett* 7(2):722–729
- Kong X, Yang X, Zhai G, et al (2020) Semantic graph based place recognition for 3d point clouds. In: Proc. IEEE/RSJ Int. Conf. Intell. Robots Syst., pp 8216–8223
- Kramer A, Harlow K, Williams C, et al (2022) Coloradar: The direct 3d millimeter wave radar dataset. *Int J Robot Res* 41(4):351–360
- Kuang H, Chen X, Guadagnino T, et al (2022) Ir-mcl: Implicit representation-based online global localization. arXiv preprint arXiv:221003113
- Kümmerle R, Grisetti G, Strasdat H, et al (2011) g2o: A general framework for graph optimization. In: Proc. IEEE Int. Conf. Robot. Autom., pp 3607–3613
- Labussière M, Laconte J, Pomerleau F (2020) Geometry preserving sampling method based on spectral decomposition for large-scale environments. *Frontiers in Robotics and AI* 7:572054
- Lai H, Yin P, Scherer S (2022) Adafusion: Visual-lidar fusion with adaptive weights for place recognition. *IEEE Robot Autom Lett*
- Latif Y, Cadena C, Neira J (2013) Robust loop closing over time for pose graph slam. *Int J Robot Res* 32(14):1611–1626
- Lee K, Lee J, Park J (2022) Learning to register unbalanced point pairs. arXiv preprint arXiv:220704221
- Lepetit V, Moreno-Noguer F, Fua P (2009) Epnp: An accurate $\mathcal{O}(n)$ solution to the pnp problem. *Int J Comput Vis* 81:155–166. <https://doi.org/10.1007/s11263-008-0152-6>
- Li J, Lee GH (2019) Usip: Unsupervised stable interest point detection from 3d point clouds. In: Proc. IEEE Conf. Comput. Vis. Pattern Recognit., pp 361–370

- Li L, Kong X, Zhao X, et al (2021a) Ssc: Semantic scan context for large-scale place recognition. In: Proc. IEEE/RSJ Int. Conf. Intell. Robots Syst., pp 2092–2099
- Li L, Kong X, Zhao X, et al (2022) Rinet: Efficient 3d lidar-based place recognition using rotation invariant neural network. *IEEE Robot Autom Lett* 7(2):4321–4328
- Li X, Pontes JK, Lucey S (2021b) Pointnetlk revisited. In: Proc. IEEE Conf. Comput. Vis. Pattern Recognit., pp 12763–12772
- Li Z, Hoiem D (2017) Learning without forgetting. *IEEE Trans Pattern Anal Mach Intell* 40(12):2935–2947
- Lim H, Hwang S, Myung H (2021) Eraser: Egocentric ratio of pseudo occupancy-based dynamic object removal for static 3d point cloud map building. *IEEE Robot Autom Lett* 6(2):2272–2279
- Lin CE, Song J, Zhang R, et al (2022) Se (3)-equivariant point cloud-based place recognition. In: 6th Annual Conference on Robot Learning
- Liu T, hai Liao Q, Gan L, et al (2021) The role of the hercules autonomous vehicle during the covid-19 pandemic: An autonomous logistic vehicle for contactless goods transportation. *IEEE Robot Autom Mag* 28(1):48–58
- Liu Z, Suo C, Zhou S, et al (2019a) Seqlpd: Sequence matching enhanced loop-closure detection based on large-scale point cloud description for self-driving vehicles. In: Proc. IEEE/RSJ Int. Conf. Intell. Robots Syst., pp 1218–1223
- Liu Z, Zhou S, Suo C, et al (2019b) Lpd-net: 3d point cloud learning for large-scale place recognition and environment analysis. In: Proc. IEEE Conf. Comput. Vis. Pattern Recognit., Seoul, Korea, pp 2831–2840
- Lowe DG (1999) Object recognition from local scale-invariant features. In: Proc. IEEE Int. Conf. Comput. Vis., pp 1150–1157
- Lowry S, Sünderhauf N, Newman P, et al (2015) Visual place recognition: A survey. *IEEE Trans Robot* 32(1):1–19
- Lu S, Xu X, Yin H, et al (2022) One ring to rule them all: Radon sinogram for place recognition, orientation and translation estimation. *arXiv preprint arXiv:220407992*
- Luo L, Cao SY, Han B, et al (2021) Bvmatch: Lidar-based place recognition using bird’s-eye view images. *IEEE Robot Autom Lett* 6(3):6076–6083
- Lusk PC, Fathian K, How JP (2021) Clipper: A graph-theoretic framework for robust data association. In: Proc. IEEE Int. Conf. Robot. Autom., pp 13828–13834
- Ma J, Chen X, Xu J, et al (2022a) Seqot: A spatial-temporal transformer network for place recognition using sequential lidar data. *arXiv preprint arXiv:220907951*

- Ma J, Zhang J, Xu J, et al (2022b) Overlaptransformer: An efficient and rotation-invariant transformer network for lidar-based place recognition. arXiv preprint arXiv:220303397
- Maddern W, Pascoe G, Linegar C, et al (2017) 1 year, 1000 km: The oxford robotcar dataset. *Int J Robot Res* 36(1):3–15
- Magnusson M, Andreasson H, Nuchter A, et al (2009a) Appearance-based loop detection from 3d laser data using the normal distributions transform. In: *Proc. IEEE Int. Conf. Robot. Autom.*, pp 23–28
- Magnusson M, Andreasson H, Nüchter A, et al (2009b) Automatic appearance-based loop detection from three-dimensional laser data using the normal distributions transform. *J Field Robot* 26(11-12):892–914
- Mangelson JG, Dominic D, Eustice RM, et al (2018) Pairwise consistent measurement set maximization for robust multi-robot map merging. In: *Proc. IEEE Int. Conf. Robot. Autom.*, pp 2916–2923
- Merfels C, Stachniss C (2016) Pose fusion with chain pose graphs for automated driving. In: *Proc. IEEE/RSJ Int. Conf. Intell. Robots Syst.*, pp 3116–3123
- Milford M, Shen C, Lowry S, et al (2015) Sequence searching with deep-learned depth for condition-and viewpoint-invariant route-based place recognition. In: *CVPR Workshop*, pp 18–25
- Milford MJ, Wyeth GF (2012) Seqslam: Visual route-based navigation for sunny summer days and stormy winter nights. In: *Proc. IEEE Int. Conf. Robot. Autom.*, pp 1643–1649
- Milioto A, Vizzo I, Behley J, et al (2019) Rangenet++: Fast and accurate lidar semantic segmentation. In: *Proc. IEEE/RSJ Int. Conf. Intell. Robots Syst.*, pp 4213–4220
- Millane A, Oleynikova H, Nieto J, et al (2019) Free-space features: Global localization in 2d laser slam using distance function maps. In: *Proc. IEEE/RSJ Int. Conf. Intell. Robots Syst.*, pp 1271–1277
- Montemerlo M, Roy N, Thrun S (2003) Perspectives on standardization in mobile robot programming: The carnegie mellon navigation (carmen) toolkit. In: *Proc. IEEE/RSJ Int. Conf. Intell. Robots Syst.*, pp 2436–2441
- Naseer T, Burgard W, Stachniss C (2018) Robust visual localization across seasons. *IEEE Trans Robot* 34(2):289–302
- Nielsen K, Hendebj G (2022) Survey on 2d lidar feature extraction for underground mine usage. *IEEE Trans Autom Sci Eng*

- Nobili S, Tinchev G, Fallon M (2018) Predicting alignment risk to prevent localization failure. In: Proc. IEEE Int. Conf. Robot. Autom., pp 1003–1010
- Oertel A, Cieslewski T, Scaramuzza D (2020) Augmenting visual place recognition with structural cues. *IEEE Robot Autom Lett* 5(4):5534–5541
- Olson E (2011) Apriltag: A robust and flexible visual fiducial system. In: Proc. IEEE Int. Conf. Robot. Autom., pp 3400–3407
- Olson E, Walter MR, Teller SJ, et al (2005) Single-cluster spectral graph partitioning for robotics applications. In: Proc. Robot., Sci. Syst. Conf., pp 265–272
- Pan Y, Xiao P, He Y, et al (2021a) Mulls: Versatile lidar slam via multi-metric linear least square. In: Proc. IEEE Int. Conf. Robot. Autom., pp 11633–11640
- Pan Y, Xu X, Li W, et al (2021b) Coral: Colored structural representation for bi-modal place recognition. In: Proc. IEEE/RSJ Int. Conf. Intell. Robots Syst., pp 2084–2091
- Pattabiraman B, Patwary MMA, Gebremedhin AH, et al (2015) Fast algorithms for the maximum clique problem on massive graphs with applications to overlapping community detection. *Internet Mathematics* 11(4-5):421–448
- Paul R, Newman P (2010) Fab-map 3d: Topological mapping with spatial and visual appearance. In: Proc. IEEE Int. Conf. Robot. Autom., pp 2649–2656
- Pepperell E, Corke PI, Milford MJ (2014) All-environment visual place recognition with smart. In: Proc. IEEE Int. Conf. Robot. Autom., IEEE, pp 1612–1618
- Pitropov M, Garcia DE, Rebello J, et al (2021) Canadian adverse driving conditions dataset. *Int J Robot Res* 40(4-5):681–690
- Pomerleau F, Colas F, Siegwart R, et al (2015) A review of point cloud registration algorithms for mobile robotics. *Foundations and Trends® in Robotics* 4(1):1–104
- Pramatarov G, De Martini D, Gadd M, et al (2022) Boxgraph: Semantic place recognition and pose estimation from 3d lidar. *arXiv preprint arXiv:220615154*
- Pretto A, Aravecchia S, Burgard W, et al (2020) Building an aerial-ground robotics system for precision farming: an adaptable solution. *IEEE Robot Autom Mag* 28(3):29–49
- Qi CR, Su H, Mo K, et al (2017) Pointnet: Deep learning on point sets for 3d classification and segmentation. In: Proc. IEEE Conf. Comput. Vis. Pattern Recognit., pp 652–660
- Qiao Z, Hu H, Shi W, et al (2021) A registration-aided domain adaptation network for 3d point cloud based place recognition. In: Proc. IEEE/RSJ Int. Conf. Intell. Robots Syst., pp 1317–1322

- Ratz S, Dymczyk M, Siegwart R, et al (2020) Oneshot global localization: Instant lidar-visual pose estimation. In: Proc. IEEE Int. Conf. Robot. Autom., pp 5415–5421
- Röhling T, Mack J, Schulz D (2015) A fast histogram-based similarity measure for detecting loop closures in 3-d lidar data. In: Proc. IEEE/RSJ Int. Conf. Intell. Robots Syst., pp 736–741
- Rosen DM, Doherty KJ, Terán Espinoza A, et al (2021) Advances in inference and representation for simultaneous localization and mapping. *Annual Review of Control, Robotics, and Autonomous Systems* 4:215–242
- Rublee E, Rabaud V, Konolige K, et al (2011) Orb: An efficient alternative to sift or surf. In: 2011 International conference on computer vision, pp 2564–2571
- Rusu RB, Blodow N, Beetz M (2009) Fast point feature histograms (fpfh) for 3d registration. In: Proc. IEEE Int. Conf. Robot. Autom., Kobe, Japan, pp 3212–3217, <https://doi.org/10.1109/ROBOT.2009.5152473>
- Saarinen J, Andreasson H, Stoyanov T, et al (2013) Normal distributions transform monte-carlo localization (ndt-mcl). In: Proc. IEEE/RSJ Int. Conf. Intell. Robots Syst., pp 382–389
- Salti S, Tombari F, Di Stefano L (2014) Shot: Unique signatures of histograms for surface and texture description. *Comput Vis Image Underst* 125:251–264
- Schaupp L, Bürki M, Dubé R, et al (2019) Oreos: Oriented recognition of 3d point clouds in outdoor scenarios. In: Proc. IEEE/RSJ Int. Conf. Intell. Robots Syst., pp 3255–3261
- Segal A, Haehnel D, Thrun S (2009) Generalized-icp. In: Proc. Robot., Sci. Syst. Conf., Seattle, WA, Seattle, WA, USA, p 435
- Shan T, Englot B, Duarte F, et al (2021) Robust place recognition using an imaging lidar. In: Proc. IEEE Int. Conf. Robot. Autom., pp 5469–5475
- Shi C, Chen X, Huang K, et al (2021) Keypoint Matching for Point Cloud Registration using Multiplex Dynamic Graph Attention Networks. *IEEE Robot Autom Lett* 6:8221–8228
- Shi S, Guo C, Jiang L, et al (2020) Pv-rcnn: Point-voxel feature set abstraction for 3d object detection. In: Proc. IEEE Conf. Comput. Vis. Pattern Recognit., pp 10529–10538
- Siegwart R, Nourbakhsh IR, Scaramuzza D (2011) Introduction to autonomous mobile robots. MIT press
- Siva S, Nahman Z, Zhang H (2020) Voxel-based representation learning for place recognition based on 3d point clouds. In: Proc. IEEE/RSJ Int. Conf. Intell. Robots

- Syst., pp 8351–8357
- Stachniss C, Burgard W (2005) Mobile robot mapping and localization in non-static environments. In: *aaai*, pp 1324–1329
- Stachniss C, Grisetti G, Burgard W (2005) Information gain-based exploration using rao-blackwellized particle filters. In: *Proc. Robot., Sci. Syst. Conf.*, pp 65–72
- Stachniss C, Leonard JJ, Thrun S (2016) Simultaneous localization and mapping. *Springer Handbook of Robotics* pp 1153–1176
- Steder B, Grisetti G, Burgard W (2010a) Robust place recognition for 3d range data based on point features. In: *Proc. IEEE Int. Conf. Robot. Autom.*, pp 1400–1405
- Steder B, Rusu RB, Konolige K, et al (2010b) Narf: 3d range image features for object recognition. In: *IROS 2010 Workshop: Defining and Solving Realistic Perception Problems in Personal Robotics*, p 2
- Sun L, Adolfsson D, Magnusson M, et al (2020) Localising faster: Efficient and precise lidar-based robot localisation in large-scale environments. In: *Proc. IEEE Int. Conf. Robot. Autom.*, pp 4386–4392
- Sünderhauf N, Protzel P (2012) Switchable constraints for robust pose graph slam. In: *Proc. IEEE/RSJ Int. Conf. Intell. Robots Syst.*, pp 1879–1884
- Tang L, Wang Y, Ding X, et al (2019) Topological local-metric framework for mobile robots navigation: a long term perspective. *Autonom Robots* 43(1):197–211
- Tang TY, De Martini D, Newman P (2021) Get to the point: Learning lidar place recognition and metric localisation using overhead imagery. *Proceedings of Robotics: Science and Systems*, 2021
- Thomas H, Qi CR, Deschaud JE, et al (2019) Kpconv: Flexible and deformable convolution for point clouds. In: *Proc. IEEE Conf. Comput. Vis. Pattern Recognit.*, pp 6411–6420
- Thrun S (2002) Probabilistic robotics. *Communications of the ACM* 45(3):52–57
- Tian Y, Chang Y, Arias FH, et al (2022) Kimera-multi: robust, distributed, dense metric-semantic slam for multi-robot systems. *IEEE Trans Robot*
- Tinchev G, Nobili S, Fallon M (2018) Seeing the wood for the trees: Reliable localization in urban and natural environments. In: *Proc. IEEE/RSJ Int. Conf. Intell. Robots Syst.*, pp 8239–8246
- Tinchev G, Penate-Sanchez A, Fallon M (2019) Learning to see the wood for the trees: Deep laser localization in urban and natural environments on a cpu. *IEEE Robot Autom Lett* 4(2):1327–1334

- Tinchev G, Penate-Sanchez A, Fallon M (2021) Skd: Keypoint detection for point clouds using saliency estimation. *IEEE Robot Autom Lett* 6(2):3785–3792
- Tipaldi GD, Arras KO (2010) Flirt-interest regions for 2d range data. In: *Proc. IEEE Int. Conf. Robot. Autom.*, pp 3616–3622
- Toft C, Maddern W, Torii A, et al (2020) Long-term visual localization revisited. *IEEE Trans Pattern Anal Mach Intell* 44(4):2074–2088
- Tolias G, Avrithis Y, Jégou H (2013) To aggregate or not to aggregate: Selective match kernels for image search. In: *Proc. IEEE Int. Conf. Comput. Vis.*, pp 1401–1408, <https://doi.org/10.1109/ICCV.2013.177>
- Tombari F, Salti S, Di Stefano L (2013) Performance evaluation of 3d keypoint detectors. *Int J Comput Vis* 102(1):198–220
- Usman M, Khan AM, Ali A, et al (2019) An extensive approach to features detection and description for 2-d range data using active b-splines. *IEEE Robot Autom Lett* 4(3):2934–2941
- Uy MA, Lee GH (2018) Pointnetvlad: Deep point cloud based retrieval for large-scale place recognition. In: *Proc. IEEE Conf. Comput. Vis. Pattern Recognit.*, pp 4470–4479
- Vaswani A, Shazeer N, Parmar N, et al (2017) Attention is all you need. *Proc Adv Neural Inf Process Syst* 30
- Vidanapathirana K, Moghadam P, Harwood B, et al (2021) Locus: Lidar-based place recognition using spatiotemporal higher-order pooling. In: *Proc. IEEE Int. Conf. Robot. Autom.*, pp 5075–5081
- Vidanapathirana K, Ramezani M, Moghadam P, et al (2022) Logg3d-net: Locally guided global descriptor learning for 3d place recognition. In: *Proc. IEEE Int. Conf. Robot. Autom.*, pp 2215–2221
- Vizzo I, Guadagnino T, Mersch B, et al (2022) Kiss-icp: In defense of point-to-point icp—simple, accurate, and robust registration if done the right way. *arXiv preprint arXiv:220915397*
- Vysotska O, Stachniss C (2019) Effective visual place recognition using multi-sequence maps. *IEEE Robot Autom Lett* 4(2):1730–1736
- Wang H, Wang C, Xie L (2020a) Intensity scan context: Coding intensity and geometry relations for loop closure detection. In: *Proc. IEEE Int. Conf. Robot. Autom.*, pp 2095–2101
- Wang W, Wang B, Zhao P, et al (2021) Pointloc: Deep pose regressor for lidar point cloud localization. *IEEE Sensors Journal* 22(1):959–968

- Wang X, Marcotte RJ, Olson E (2019) Glfp: Global localization from a floor plan. In: Proc. IEEE/RSJ Int. Conf. Intell. Robots Syst., pp 1627–1632
- Wang Y, Solomon JM (2019) Deep closest point: Learning representations for point cloud registration. In: Proc. IEEE Conf. Comput. Vis. Pattern Recognit., pp 3523–3532
- Wang Y, Sun Z, Xu CZ, et al (2020b) Lidar iris for loop-closure detection. In: Proc. IEEE/RSJ Int. Conf. Intell. Robots Syst., pp 5769–5775
- Wang Y, Sun Z, Xu CZ, et al (2020c) Lidar iris for loop-closure detection. In: Proc. IEEE/RSJ Int. Conf. Intell. Robots Syst., pp 5769–5775, <https://doi.org/10.1109/IROS45743.2020.9341010>
- Wiesmann L, Marcuzzi R, Stachniss C, et al (2022a) Retriever: Point cloud retrieval in compressed 3d maps. In: Proc. IEEE Int. Conf. Robot. Autom., pp 10925–10932
- Wiesmann L, Nunes L, Behley J, et al (2022b) Kppr: Exploiting momentum contrast for point cloud-based place recognition. *IEEE Robot Autom Lett* 8(2):592–599
- Wilbers D, Rumberg L, Stachniss C (2019) Approximating marginalization with sparse global priors for sliding window slam-graphs. In: Proc. IEEE Int. Conf. on Robot Comput., pp 25–31
- Wolcott RW, Eustice RM (2015) Fast lidar localization using multiresolution gaussian mixture maps. In: Proc. IEEE Int. Conf. Robot. Autom., pp 2814–2821
- Wurm KM, Hornung A, Bennewitz M, et al (2010) Octomap: A probabilistic, flexible, and compact 3d map representation for robotic systems. In: ICRA 2010 workshop: Best Practice in 3D Perception and Modeling for Mobile Manipulation
- Xia Y, Xu Y, Li S, et al (2021) Soe-net: A self-attention and orientation encoding network for point cloud based place recognition. In: Proc. IEEE Conf. Comput. Vis. Pattern Recognit., pp 11348–11357
- Xie Y, Zhang Y, Chen L, et al (2021) Rdc-slam: A real-time distributed cooperative slam system based on 3d lidar. *IEEE Trans Intell Transp Syst*
- Xu H, Zhang Y, Zhou B, et al (2022a) Omni-swarm: A decentralized omnidirectional visual-inertial-uwB state estimation system for aerial swarms. *IEEE Trans Robot*
- Xu TX, Guo YC, Lai YK, et al (2021a) Transloc3d: Point cloud based large-scale place recognition using adaptive receptive fields. *arXiv preprint arXiv:2105.11605*
- Xu X, Yin H, Chen Z, et al (2021b) Disco: Differentiable scan context with orientation. *IEEE Robot Autom Lett* 6(2):2791–2798

- Xu X, Lu S, Wu J, et al (2022b) Ring++: Roto-translation invariant gram for global localization on a sparse scan map. arXiv preprint arXiv:221005984
- Yan F, Vysotska O, Stachniss C (2019) Global localization on openstreetmap using 4-bit semantic descriptors. In: Proc. IEEE Eur. Conf. Mobile Robot., pp 1–7
- Yang H, Antonante P, Tzoumas V, et al (2020) Graduated non-convexity for robust spatial perception: From non-minimal solvers to global outlier rejection. *IEEE Robot Autom Lett* 5(2):1127–1134
- Yang H, Shi J, Carlone L (2021) Teaser: Fast and certifiable point cloud registration. *IEEE Trans Robot* 37(2):314–333. <https://doi.org/10.1109/TRO.2020.3033695>
- Yang J, Li H, Jia Y (2013) Go-icp: Solving 3d registration efficiently and globally optimally. In: Proc. IEEE Int. Conf. Comput. Vis., Sydney, NSW, Australia, pp 1457–1464
- Yew ZJ, Lee GH (2018) 3dfeat-net: Weakly supervised local 3d features for point cloud registration. In: Proc. Eur. Conf. Comput. Vis., pp 607–623
- Yew ZJ, Lee GH (2022) Regtr: End-to-end point cloud correspondences with transformers. In: Proc. IEEE Conf. Comput. Vis. Pattern Recognit., pp 6677–6686
- Yin H, Ding X, Tang L, et al (2017) Efficient 3d lidar based loop closing using deep neural network. In: Proc. IEEE Int. Conf. Robot. Biom, pp 481–486
- Yin H, Tang L, Ding X, et al (2018) Locnet: Global localization in 3d point clouds for mobile vehicles. In: Proc. IEEE Intell. Veh. Symp., pp 728–733
- Yin H, Tang L, Ding X, et al (2019a) A failure detection method for 3d lidar based localization. In: Proc. Chinese Autom. Congr., pp 4559–4563
- Yin H, Wang Y, Ding X, et al (2019b) 3d lidar-based global localization using siamese neural network. *IEEE Trans Intell Transp Syst* 21(4):1380–1392
- Yin H, Wang Y, Tang L, et al (2020) 3d lidar map compression for efficient localization on resource constrained vehicles. *IEEE Trans Intell Transp Syst* 22(2):837–852
- Yin H, Xu X, Wang Y, et al (2021) Radar-to-lidar: Heterogeneous place recognition via joint learning. *Frontiers in Robotics and AI* 8:661199
- Yin H, Wang Y, Wu J, et al (2022a) Radar style transfer for metric robot localisation on lidar maps. *CAAI Trans Intell Technol*
- Yin H, Lin Z, Yeoh JK (2023) Semantic localization on bim-generated maps using a 3d lidar sensor. *Automation in Construction* 146:104641

- Yin P, Wang F, Egorov A, et al (2022b) Fast sequence-matching enhanced viewpoint-invariant 3-d place recognition. *IEEE Trans Ind Electron* 69(2):2127–2135. <https://doi.org/10.1109/TIE.2021.3057025>
- Yin P, Zhao S, Cisneros I, et al (2022c) General place recognition survey: Towards the real-world autonomy age. *arXiv preprint arXiv:220904497*
- Yuan C, Lin J, Zou Z, et al (2022) Std: Stable triangle descriptor for 3d place recognition. *arXiv preprint arXiv:220912435*
- Yuan W, Eckart B, Kim K, et al (2020) Deepgmr: Learning latent gaussian mixture models for registration. In: *Proc. Eur. Conf. Comput. Vis.*, Springer, pp 733–750
- Yue Y, Zhao C, Wang Y, et al (2022) Aerial-ground robots collaborative 3d mapping in gnss-denied environments. In: *Proc. IEEE Int. Conf. Robot. Autom.*, pp 10041–10047
- Zeng A, Song S, Nießner M, et al (2017) 3dmatch: Learning local geometric descriptors from rgb-d reconstructions. In: *Proc. IEEE Conf. Comput. Vis. Pattern Recognit.*, pp 1802–1811
- Zhang J, Singh S (2014) Loam: Lidar odometry and mapping in real-time. In: *Proc. Robot., Sci. Syst. Conf.*, Berkeley, CA, pp 1–9
- Zhang W, Xiao C (2019) Pcan: 3d attention map learning using contextual information for point cloud based retrieval. In: *Proc. IEEE Conf. Comput. Vis. Pattern Recognit.*, pp 12436–12445
- Zhao S, Zhang H, Wang P, et al (2021) Super odometry: Imu-centric lidar-visual-inertial estimator for challenging environments. In: *Proc. IEEE/RSJ Int. Conf. Intell. Robots Syst.*, pp 8729–8736
- Zheng K (2021) Ros navigation tuning guide. In: *Robot Operating System (ROS)*. Springer, p 197–226
- Zhong S, Qi Y, Chen Z, et al (2022) Dcl-slam: A distributed collaborative lidar slam framework for a robotic swarm. *arXiv preprint arXiv:221011978*
- Zhou QY, Park J, Koltun V (2016) Fast global registration. In: *Proc. Eur. Conf. Comput. Vis.*, Springer, Amsterdam, the Netherlands, pp 766–782
- Zhou Z, Zhao C, Adolfsson D, et al (2021) Ndt-transformer: Large-scale 3d point cloud localisation using the normal distribution transform representation. In: *Proc. IEEE Int. Conf. Robot. Autom.*, pp 5654–5660
- Zhu M, Ghaffari M, Peng H (2022) Correspondence-free point cloud registration with so (3)-equivariant implicit shape representations. In: *Conference on Robot Learning*, PMLR, pp 1412–1422

- Zhu Y, Ma Y, Chen L, et al (2020) Gosmatch: Graph-of-semantics matching for detecting loop closures in 3d lidar data. In: Proc. IEEE/RSJ Int. Conf. Intell. Robots Syst., pp 5151–5157
- Zimmerman N, Wiesmann L, Guadagnino T, et al (2022) Robust onboard localization in changing environments exploiting text spotting. arXiv preprint arXiv:220312647
- Zimmerman N, Guadagnino T, Chen X, et al (2023) Long-Term Localization using Semantic Cues in Floor Plan Maps. IEEE Robot Autom Lett 8(1):176–183